Published in final edited form as:
*Bull Math Biol*. 2014 December ; 76(12): 2945–2984. doi:10.1007/s11538-014-0040-x.

# Piecewise linear and Boolean models of chemical reaction networks

**Alan Veliz-Cuba**[*,a,b], **Ajit Kumar**[a,c], and **Krešimir Josić**[a,d]

Ajit Kumar: ajit.kumar@snu.edu.in; Krešimir Josić: josic@math.uh.edu

[a]Department of Mathematics, University of Houston, Houston, Texas 77204-3008, USA

[b]Department of Biochemistry and Cell Biology, Rice University, Houston, Texas 77251-1892, USA

[c]Department of Mathematics, Shiv Nadar Univerisity, Greater Noida, Uttar Pradesh 203207, India

[d]Department of Biology and Biochemistry, University of Houston, Houston, Texas 77204-5001, USA

## Abstract

Models of biochemical networks are frequently complex and high-dimensional. Reduction methods that preserve important dynamical properties are therefore essential for their study. Interactions in biochemical networks are frequently modeled using Hill functions ($x^n/(J^n + x^n)$). Reduced ODEs and Boolean approximations of such model networks have been studied extensively when the exponent $n$ is large. However, while the case of small constant $J$ appears in practice, it is not well understood. We provide a mathematical analysis of this limit, and show that a reduction to a set of piecewise linear ODEs and Boolean networks can be mathematically justified. The piecewise linear systems have closed form solutions that closely track those of the fully nonlinear model. The simpler, Boolean network can be used to study the qualitative behavior of the original system. We justify the reduction using geometric singular perturbation theory and compact convergence, and illustrate the results in network models of a toggle switch and an oscillator.

### Keywords

Piecewise linear models; Boolean models; steady state analysis; biochemical networks

## 1 Introduction

Accurately describing the behavior of interacting enzymes, proteins, and genes requires spatially extended stochastic models. However, such models are difficult to implement and fit to data. Hence simplified models are frequently used instead. In many such models, a single ODE is used to describe changes in concentration of a species (a node in the network), and sigmoidal functions to describe interactions between them. Even such

[*]Correspondence Author: Alan Veliz-Cuba (alanavc@math.uh.edu), phone: 1-713-743-3490, fax: 1-713-743-3505.
MSC: 92C42, 37N25, 94C10

simplified ODEs are typically intractable. The number of parameters and the potential dynamical complexity make it difficult to fully analyze the systems using only numerical methods. Reduced models that capture the overall dynamics, or allow approximate solutions are of great help in this situation [Verhulst (2006); Hek (2010)].

An analytical treatment is possible in certain limits. Three main approaches have been developed to analyze models of biochemical interaction networks [Polynikis et al. (2009)]: *Quasi Steady State Approximations* (QSSA), *Piecewise Linear Approximations* (PLA), and *discretizations of continuous time ODEs*.

In certain limits, interactions between network elements become switch–like [Kauffman (1969); Glass (1975,b); Snoussi (1989); Mochizuki (2005); Alon (2006); Mendoza and Xenarios (2006); Davidich and Bornholdt (2008); Wittmann et al. (2009); Franke (2010); Veliz-Cuba et al. (2012); Casey et al. (2006); Sun et al. (2013)]. For example, the Hill function, $f(x) = x^n/(x^n + J^n)$, approaches the Heaviside function, $H(x - J)$, in the limit of large $n$, and the domain on which the network is modeled is naturally split into subdomains. The threshold, corresponding to the parameter $J$ in the Hill function, divides the domain into two subdomains within which the Heaviside function is constant. Within each subdomain a node is either fully expressed, or not expressed at all. When $n$ is large, the Hill function, $f(x)$, is approximately constant in each of the subdomains, and boundary layers occur when $x$ is close to the threshold, $x \approx J$ [Ironi et al. (2011)].

To simplify the system further, we can map values of $x$ below the threshold to 0, and the values above the threshold to 1 to obtain a *Boolean network* (BN), a map

$$h=(h_1,\ldots,h_N):\{0,1\}^N \to \{0,1\}^N,$$

where each function $h_i$ describes how variable $i$ qualitatively depends on the other variables [Glass and Kauffman (1973); Snoussi (1989); Thomas and D'Ari (1990); Albert and Othmer (2003); Mendoza and Xenarios (2006); Davidich and Bornholdt (2008); Abou-Jaoudé et al. (2009, 2010); Wittmann et al. (2009); Franke (2010); Veliz-Cuba et al. (2012); Cheng et al. (2013); Sun et al. (2013)]. Such reduced systems are simpler to analyze, and share the dynamical properties of the original system, if the reduction is done properly.

The reduced models obtained in the limit of a large Hill coefficient, $n$, have a long and rich history. Piecewise linear functions of the form proposed in [Glass and Kauffman (1973)] have been shown to be well suited for the modeling of biochemical regulatory networks, and can sometimes be justified rigorously [De Jong et al. (2004)]. In particular, singular perturbation theory can be used to obtain reduced equations within each subdomain and the boundary layers, and global approximations within the entire domain [Ironi et al. (2011)]. On the other hand, although BNs have been used to model the dynamics of different biological systems, their relation to more complete models was demonstrated mainly in case studies, heuristically or only for steady states [Glass and Kauffman (1973); Glass (1975,b); Snoussi (1989); Thomas and D'Ari (1990); Albert and Othmer (2003); Mendoza and Xenarios (2006); Davidich and Bornholdt (2008); Abou-Jaoudé et al. (2009, 2010);

Wittmann et al. (2009); Franke (2010); Veliz-Cuba et al. (2012); Chaves et al. (2010); Edwards et al. (2001); Sun et al. (2013)].

Here we again model interactions between nodes using the Hill function, $x^n/(x^n + J^n)$. However, instead of assuming that $n$ is large, we assume that $J$ is small. Although the subsequent results hold for any fixed $n$, for simplicity we assume $n = 1$ (see the Appendix for a comment about the case $n > 1$).

More precisely, we consider a model biological network where the activity at each of the $N$ nodes is described by $u_i \in [0, 1]$, and evolves according to

$$\frac{du_i}{dt} = A_i \frac{1 - u_i}{J + 1 - u_i} - I_i \frac{u_i}{J + u_i}, \quad (1)$$

where $J > 0$, and the functions $A_i = A_i(u)$, $I_i = I_i(u)$ are affine and nonnegative. The parameter $J$ could be different for each term in each equation, but the arguments and proofs do not change; so for simplicity we assume that all $J$'s are equal.

Here $A_i$ and $I_i$ describe how other variables affect $u_i$ and can represent the strength of activation/phosphorylation/production and inhibition/dephosphorylation/decay, respectively. The variables $u_i$ can represent species such as protein concentrations, the active form of enzymes, or activation level of genes. It is easy to show that the region $0 \le u_i \le 1$, $1 \le i \le N$ is invariant and Eq. (1) describes a system of equations whose solutions are constrained to $[0, 1]^N$. Equations involving this special class of Hill functions are generally referred to as Michaelis-Menten type equations, and $J$ the Michaelis-Menten constant [Michaelis and Menten (1913); Goldbeter and Koshland (1981); Goldbeter (1991); Novak and Tyson (1993); Novak et al. (2001); Tyson et al. (2003); Ciliberto et al. (2007); Davidich and Bornholdt (2008); Ma et al. (2009)].

This type of model has been used widely [Goldbeter and Koshland (1981); Novak et al. (1998); Goldbeter (1991); Novak et al. (2001); De Jong (2002); Tyson et al. (2003); Ishii et al. (2007); Ciliberto et al. (2007); Davidich and Bornholdt (2008); van Zwieten et al. (2011)]. An important example is provided by a protein that can exist in an unmodified form, $W$, and a modified form, $W^*$, (e.g. proteases, and Cdc2, Cdc25, Wee1, and Mik1 kinases [Goldbeter (1991); Novak et al. (1998, 2001)]) where the conversion between the two forms is catalyzed by two enzymes, $E_1$ and $E_2$ [Goldbeter and Koshland (1981); Goldbeter (1991); Novak et al. (1998, 2001)]. However, the models of chemical reactions we consider can be rigorously derived from the Chemical Master Equation only in the case of a single reaction [Kumar and Josić (2011)]. The starting point of our reduction should therefore be regarded as phenomenological models of the system (see Appendix for details).

The case of small $J$ has a simple physical interpretation in the case of models of enzymatic reactions: Consider the Hill function that appears in the Michaelis-Menten reduction scheme, which models the catalysis of the inactive form of some protein to its active form in the presence of an enzyme. When $J$ is small the total enzyme concentration is much smaller than the total protein concentration. Also, the constant $J$ is frequently very small in

published models of biological networks [Novak et al. (2001); Davidich and Bornholdt (2008)], which further motivates examining Eq. (1) when $0 < J \ll 1$.

We discuss a two step reduction

$$\text{full, nonlinear model} \rightarrow \text{piecewise linear model (PL)} \rightarrow \text{Boolean Network (BN)}.$$

We first illustrate this reduction using two standard examples, and then provide a general mathematical justification. We note that the reduction obtained in the first step (see Eq. (14a)) is actually (algebraic) piecewise affine. However, it is customary to refer to the equation and the associated model as *piecewise linear* [Glass and Kauffman (1973); Snoussi (1989); Thomas and D'Ari (1990); De Jong (2002)]. We follow this convention.

The main idea behind the piecewise linear (PL) reduction is simple: If $J \ll x$ then the Hill functions, $f(x) = x/(x+J) \approx 1$. However, when $x$ and $J$ are comparable, $x \sim J$, this is no longer true. In this boundary layer, we rescale variables by introducing $\tilde{x} := x/J$. A similar argument works for the function $(1 - x)/(J + 1 - x)$ (see Appendix). We show that using this observation, the domain $[0, 1]^N$ naturally decomposes into a nested sequence of hypercubes. The dynamics on each hypercube is described by a solvable differential-algebraic system of equations. The PL reduction therefore gives an *analytically tractable* approximate solution to the original system.

In the next step of the reduction we obtain a Boolean Network (BN): The PL approximation is used to divide $[0, 1]^N$ into chambers. Within nearly all of a chamber the rate of change of each element of the network is constant when $J \ll 1$. We use these chambers to define a BN. A similar approach was used to motivate a Boolean reduction of a model protein interaction network [Davidich and Bornholdt (2008)].

The mathematical justification also follows two steps. We use Geometric Singular Perturbation Theory (GSPT) in Section 4.1 to justify the PL approximation. The justification of the BN reduction is given in Section 4.2. We show that there is a one-to-one correspondence between steady states (equilibrium solutions) of the BN and the full and PL system near the vertices of $[0, 1]^N$. Futhermore, we show that this one-to-one correspondence between steady states is actually global (up to a set of small measure in $[0, 1]^N$). BNs have been used to study oscillatory behavior [Li et al. (2004); Abou-Jaoudé et al. (2009)], and we prove in Section 4.2.3 that under some conditions oscillations in a BN correspond to oscillations in the full system.

## 2 Examples

We start by demonstrating the main idea of our approach using networks of two and three mutually repressing nodes. These nodes can represent genes that mutually inhibit each other [Gardner et al. (2000); Elowitz and Leibler (2000)]. We remark that, although these genetic networks have been modeled in the past by Hill functions and decay terms, the systems we consider here can be used as phenomenological models of biochemical networks, and have been used as models in the case of enzyme activation/phosphorylation (Goldbeter and

Koshland, 1981; Novak et al., 1998; Goldbeter, 1991; Novak et al., 2001; De Jong, 2002; Tyson et al., 2003; Ishii et al., 2007; Ciliberto et al., 2007; Davidich and Bornholdt, 2008; van Zwieten et al., 2011). Thus, the theory we develop applies whenever the model given in Eq. (1) is applicable. We accompany these examples with a heuristic explanation of the different steps in the reduction.

### 2.1 A network of two mutually inhibiting elements

We start with the common *toggle switch* motif, *i. e* a network of two mutually repressing elements (see Fig. 1a) [Tyson et al. (2003); Gardner et al. (2000)]. Let $(u_1, u_2) \in [0, 1]^2$ represent the normalized levels of activity at the two nodes. Therefore, when $u_i = 1$ the $i^{\text{th}}$ network element is maximally active (expressed). The activity of the two nodes in the system can be modeled by

$$\begin{aligned}\frac{du_1}{dt}&=0.5\frac{1-u_1}{J+1-u_1}-u_2\frac{u_1}{J+u_1},\\ \frac{du_2}{dt}&=0.5\frac{1-u_2}{J+1-u_2}-u_1\frac{u_2}{J+u_2},\end{aligned} \quad (2)$$

where $J$ is some positive constant. The structure of Eq. (2) implies that the cube $[0, 1]^2 = \{(u_1, u_2) \mid 0 \le u_1, u_2 \le 1\}$ is invariant (see Proposition 1).

**2.1.1 Piecewise linear approximation—**In the limit of small $J$, Eq. (2) can be approximated by a piecewise linear differential equation: If $u_i$ is not too close to zero the expression $u_i/(J + u_i)$ is approximately unity. More precisely, we fix a small $\delta > 0$, which will be chosen to depend on $J$. When $u_i > \delta$ and $J$ is small then $u_i/(J + u_i) \approx 1$. Similarly, when $u_i < 1 - \delta$ and $J$ is small then $(1 - u_i)/(J + 1 - u_i) \approx 1$.

With this convention in mind we break the cube $[0, 1]^2$ into several subdomains, and define a different reduction of Eq. (2) within each. Let $\mathscr{R}_S^T$ denote the region where $S$ is the set of variables that are close to 0, and $T$ is the set of variables close to 1 (See Eq. (12)). We will omit the curly brackets and commas in $\mathscr{R}_S^T$ (e.g $\mathscr{R}_{\{\}}^{\{\}}=\mathscr{R}$ and $\mathscr{R}_{\{1\}}^{\{\}}=\mathscr{R}_1$) and (see Fig. 2a).

We first reduce Eq. (2) on each of the subdomains. The interior domain of $[0, 1]^2$ consist of points where neither coordinate is close to 0 nor 1, and is defined by

$$\mathscr{R}:=\{(u_1,u_2)\in[0,1]^2|\delta\le u_1\le 1-\delta \text{ and } \delta\le u_2\le 1-\delta\}. \quad (3)$$

Eq. (2), restricted to $\mathscr{R}$ is approximated by the linear differential equation

$$\frac{du_1}{dt}=0.5-u_2, \quad \frac{du_2}{dt}=0.5-u_1. \quad (4)$$

On the other hand, if one of the coordinates is near the boundary, while the other is in the interior, the approximation is different. For instance, the region

$$\mathscr{R}_2:=\{(u_1,u_2)\in[0,1]^2|u_2<\delta \text{ and } \delta\le u_1\le 1-\delta\}, \quad (5)$$

forms a boundary layer where $u_2$ is of the same order as $J$.

The term $u_2/(J + u_2)$ cannot be approximated by unity. Instead the approximation takes the form

$$\frac{du_1}{dt}=0.5, \quad (6a)$$

$$\frac{du_2}{dt}=0.5-u_1\frac{u_2}{J+u_2}. \quad (6b)$$

This equation can be simplified further. For simplicity we work on $\mathscr{R}_2 \cap \{u{:}u_1{>}.5\}$. Let $(u_1(0), u_2(0)) \in \mathscr{R}_2 \cap \{u{:}u_1{>}.5\}$ and consider $u_2^*(t)$ such that $0.5-u_1(t)u_2^*(t)/(J+u_2^*(t))=0$; that is, $u_2^*(t)$ is defined so that $(u_1(t), u_2^*(t))$ is on the nullcline of Eq. (6). It can be shown that if $u_2(t)>u_2^*(t)$ then $du_2/dt < 0$, and if $u_2(t)<u_2^*(t)$ then $du_2/dt > 0$. Therefore, $u_2(t)$ approaches $u_2^*(t)$ as $t$ increases. Thus, if $(u_1(t), u_2(t))$ is rapidly driven to this nullcline, then we can approximate Eq. (6) with

$$\frac{du_1}{dt}=0.5, \quad (7a)$$

$$0=0.5-u_1\frac{u_2}{J+u_2}. \quad (7b)$$

Note that Eq. (7a) is linear and decoupled from Eq. (7b), while Eq. (7b) is an algebraic system which can be solved to obtain $u_2 \approx J/(2u_1 - 1)$. Within $\mathscr{R}_2$ we thus obtain the approximation

$$u_1(t)=0.5t+u_1(0) \quad (8a)$$

$$u_2(t)=\frac{J}{t+2u_1(0)-1} \quad (8b)$$

We only have the freedom of specifying the initial condition $u_1(0)$, since $u_2(0)$ is determined by the solution of the algebraic equation (7b). As we explain below, this algebraic equation defines a slow manifold within the subdomain $\mathscr{R}_2$. The reduction assumes that solutions are instantaneously attracted to this manifold.

Table 1 shows how this approach can be extended to all of $[0, 1]^2$. There are 9 subdomains of the square, one corresponding to the interior and four each to the edges and vertices. On the latter eight subdomains, one or both variables are close to either 0 or 1. Following the preceding arguments, variable(s) close to 0 or 1 can be described by an algebraic equation. The resulting algebraic-differential systems are given in the last column of Table 1. Furthermore, using $u_i(t) \approx 0$ for $i \in S$ and $u_i(t) \approx 1$ for $i \in T$, we obtain a simple approximation of the dynamics in each subdomain which is 0-th order in $J$. For example, in $\mathscr{R}_2$, we obtain the approximation $u_1(t) \approx 0.5t + u_1(0)$, $u_2(t) \approx 0$.

Each approximate solution can exit the subdomain within which it is defined if at some time $u_i \approx 0$ or $u_i \approx 1$ and the $i$-th coordinate of the vector field is positive or negative, respectively. This can happen when the sign of some entry of the vector field changes. Thus solutions can exit subdomains when they reach a nullcline. The global approximate solution of Eq. (2) is obtained by using the exit point from one subdomain as the initial condition for the approximation in the next. In subdomains other than $\mathscr{R}$ some of the initial conditions will be prescribed by the algebraic part of the reduced system. The global approximation may therefore be discontinuous, as solutions entering a new subdomain are assumed to instantaneously jump to the slow manifold defined by the algebraic part of the reduced system. This discontinuity may be overcome by "gluing" pieces of the solutions using matched asymptotics (especially when specific models are studied); however, since the discontinuity "jump" is negligible as $J \to 0$, this approach provides a good approximation (Fig. 3ab)). Furthermore, the 0-th order approximation (i.e. the limit of the approximation as $J \to 0$) will be continuous (Fig. 3c).

**2.1.2 Boolean approximation—**We now derive a Boolean approximation, $h = (h_1, h_2) : \{0, 1\}^2 \to \{0, 1\}^2$, that captures certain qualitative features of Eq. (2). The idea is to project small values of $u_i$ to 0 and large values of $u_i$ to 1, and map the value of the $i$-th variable into 0 and 1 depending on whether $u_i$ is decreasing or increasing, respectively. We will show that the resulting BN can be used directly to detect steady states in the corner subdomains.

Note that for a BN time is discrete; a time step in the Boolean approximation can be interpreted as the time it takes the original system to transition between different regions of $[0, 1]^2$. Different transitions in the Boolean network may have different duration in the original system; so the time steps in the BN are only used to keep track of the sequence of events, but not their duration.

The reduction described in the previous section gives a linear ODE in the interior region $\mathscr{R}$ (Eq. (4)). Since $\mathscr{R}$ approaches $[0, 1]^2$ as $J \to 0$, the approximating linear system provides significant information about the behavior of the full, nonlinear system for $J$ small.

We first examine the nullclines. In Fig. 4 we can see that as $J$ decreases, in the interior of $[0, 1]^2$ the nullclines of Eq. (2) approach the nullclines of Eq. (4) given by $u_2 = .5$ and $u_1 = .5$ restricted to $[0, 1]^2$. These lines divide the domain into four chambers (Fig. 2b), which we denote

$$\mathscr{C}_{12}:=[0,0.5)\times[0,0.5),\quad \mathscr{C}_1^2:=[0,0.5)\times(0.5,1],\quad \mathscr{C}_2^1:=(0.5,1]\times[0,0.5),\quad \mathscr{C}^{12}:=(0.5,1]\times(0.5,1].$$

On the other hand, the part of the nullclines inside the boundary subdomains are approximately the slow manifolds defined by equivalents of Eq. (8b). Here the slow manifolds converge to the nullclines as $J \to 0$ (See Fig. 4).

We consider Eq. (2) in each chamber, starting with the first coordinate, $u_1(t)$. For any solution with initial condition in $\mathscr{C}_{12}$, the sign of $u_1'(0)$ is positive and $u_1(t)$ increases within the chamber. We use this observation to define $h_1(\mathscr{C}_{12})=1$. The formal definition of this

function will be given below – intuitively $h_i(\cdot)$ maps a chamber to 1 if $u_i$ is increasing within the chamber, and to 0 otherwise. Similarly, since $u_1(t)$ initially increases within $\mathscr{C}_2^1$, we let $h_1(\mathscr{C}_2^1)=1$. Similarly we set $h_1(\mathscr{C}^{12})=0$, $h_1(\mathscr{C}_1^2)=0$, $h_2(\mathscr{C}_{12})=1$, $h_2(\mathscr{C}_1^2)=1$, $h_2(\mathscr{C}_2^1)=0$, and $h_2(\mathscr{C}^{12})=0$. The *i*-th variable is "discretized," *i.e.* mapped to 0 and 1 depending on whether $u_i$ is decreasing or increasing, respectively.

More formally, consider the set $\{0, 1\}^2$, with each element, $(i, j)$, identified with a chamber (e.g., the element (0, 1) represents the chamber $\mathscr{C}_1^2$). Then $h_1$ and $h_2$ are defined as Boolean functions from $\{0, 1\}^2$ to $\{0, 1\}$ by setting $h_1$ (0, 0) = 1, $h_1$ (0, 1) = 0, $h_1$ (1, 0) = 1, $h_1$ (1, 1) = 0, and $h_2$ (0, 0) = 1, $h_2$ (0, 1) = 1, $h_2$ (1, 0) = 0, $h_2$ (1, 1) = 0. These two Boolean functions define a BN, $h = (h_1, h_2) : \{0, 1\}^2 \to \{0, 1\}^2$. The functions also define a dynamical system, $x(t + 1) = h(x(t))$, $x \in \{0, 1\}^2$.

The BN reduction can be obtained easily from the sign (evaluated coordinate-wise) of $(.5 - u_2, .5 - u_1)$ at the vertices of $[0, 1]^2$, since the sign of the vector field is constant within a chamber. To do so we use the the Heaviside function, $H$, defined by $H(y) = 0$ if $y < 0$, $H(y) = 1$ if $y > 0$, and $H(0)=\frac{1}{2}$. For example, in $\mathscr{C}_{12}$, both entries increase. We can see this by evaluating $H(.5 - u_2) = H(.5 - u_1) = 1$ for $u = (0, 0)$. Using the same argument in each chamber, we obtain the BN

$$h(x)=H(.5-x_2,.5-x_1), \quad (9)$$

where we used the convention that $H$ acts entry-wise on each component in the argument.

**2.1.3 Steady states of the BN and the PL approximation—**While the BN gives information about which variables increase and decrease within a chamber, it is not yet clear how or if the dynamics of the BN in Eq. (9), and the PL approximation in Table 1 are related.

We next show that the steady states of the PL approximation near the vertices can be determined by the steady states of the BN. The reduced equations in the corner subdomains $\mathscr{R}_{12}$, $\mathscr{R}^{12}$, $\mathscr{R}_1^2$, and $\mathscr{R}_2^1$ are purely algebraic. When $J$ is small, some of these equations have a solution in $[0, 1]^2$, indicating a stable fixed point near the corresponding corner (in this case $\mathscr{R}_2^1$ and $\mathscr{R}_2^1$). Others will not have a solution in $[0, 1]^2$, indicating that solutions do not enter the corresponding subdomain (here $\mathscr{R}_{12}$ and $\mathscr{R}^{12}$). Solutions that start in these subdomains will leave. To make the relationship between steady states less dependent on the actual parameters, consider the system

$$\begin{aligned}\frac{du_1}{dt}&=b_1^+\frac{1-u_1}{J+1-u_1}-(u_2+b_1^-)\frac{u_1}{J+u_1},\\ \frac{du_2}{dt}&=b_2^+\frac{1-u_2}{J+1-u_2}-(u_1+b_2^-)\frac{u_2}{J+u_2},\end{aligned}$$

where $x^+ = \max\{x, 0\}$ and $x^- = \max\{-x, 0\}$ (note that $x = x^+ - x^-$). In the previous example $b_1 = b_2 = .5$, $b_1^+=b_2^+=.5$ and $b_1^-=b_2^-=0$.

Now, at the corner subdomain $\mathscr{R}_{12}$ we have the approximate equations,

$$0=b_1^+ - b_1^- \frac{u_1}{J+u_1}, 0=b_2^+ - b_2^- \frac{u_2}{J+u_2},$$

or equivalently,

$$u_1=\frac{-b_1^+ J}{b_1}, u_2=\frac{-b_2^+ J}{b_2}.$$

These equations have a solution in $\mathscr{R}_{12}$ if and only if $b_1 < 0$ and $b_2 < 0$, or equivalently, if and only if $H(b_1, b_2) = (0, 0)$. A similar analysis leads to the following conditions for the existence of fixed points in each corner subdomain

$$\begin{array}{ll} \text{On } \mathscr{R}_{12}: H(b_1,b_2)=(0,0), & \text{On } \mathscr{R}^{12}: H(b_1-1,b_2-1)=(1,1), \\ \text{On } \mathscr{R}_1^2: H(b_1-1,b_2)=(0,1), & \text{On } \mathscr{R}_2^1: H(b_1,b_2-1)=(1,0). \end{array}$$

More compactly, the condition is $H(b_1 - x_2, b_2 - x_1) = (x_1, x_2)$, where $x = (x_1, x_2)$ is the corner of interest. Hence, the BN can also be used to detect which corner subdomains contain steady states.

The relationship between steady states in the full system at the corner subdomains and the steady states of the BN is straightforward. However, since there are many update schemes for BNs, the relationship between trajectories is more subtle. For example, using synchronous updates we obtain the transition $(0, 0) \to (1, 1)$ which is not compatible with the solutions of Eq. (2) (See Fig. 5). On the other hand, using asynchronous update we obtain the transitions $(0, 0) \to (1, 0)$ and $(0, 0) \to (0, 1)$, which are more representative of the solutions of Eq. (2). Thus, we will focus on transitions that are independent of the update scheme, that is, transitions where only one entry changes.

### 2.2 A network of three mutually inhibiting elements

The same reduction can be applied to systems of arbitrary dimension. As an example consider the *repressilator* motif, *i.e.* a network of three elements where one is inhibited by another one (see Fig. 1a) [Tyson et al. (2003); Elowitz and Leibler (2000)]. As mentioned at the beginning of the section, this model is phenomenological. The model is described by

$$\begin{array}{l} \frac{du_1}{dt}=0.6\frac{1-u_1}{J+1-u_1} - u_3\frac{u_1}{J+u_1}, \\ \frac{du_2}{dt}=0.4\frac{1-u_2}{J+1-u_2} - u_1\frac{u_2}{J+u_2}, \\ \frac{du_3}{dt}=0.3\frac{1-u_3}{J+1-u_3} - u_2\frac{u_3}{J+u_3}. \end{array} \quad (10)$$

The cyclic repression of the three elements in this network leads to oscillatory solutions over a large range of values of $J$. The domain of this system, $[0, 1]^3$, can be divided into 27 subdomains corresponding to 1 interior, 6 faces, 12 edges, and 8 vertices.

We can again approximate Eq. (10) with solvable differential–algebraic equations within each subdomain, to obtain a global approximate solution; and in the limit $J \to 0$ we obtain a continuous 0-th order approximation. In contrast to the PL approximation, the 0-th order approximation does not take into consideration the specific value of $J$. However, the solution to the full system converges to the 0-th order approximation as $J \to 0$ (See Fig. 6).

Note that both the numerically obtained solution to Eq. (10) and 0-th order approximation exhibit oscillations.

In this singular limit, solutions can exit a subdomain when they reach a nullcline of the linear system. For example, when $u_2$ is close to 0 and a solution transitions from $u_1 > .4$ to $u_1 < .4$, the sign of the second entry of $(0.6 - u_3, 0.4 - u_1, 0.3 - u_2)$ changes from negative to positive; so the second coordinate of the solution starts increasing (see Fig. 6, panel (e)). Solutions therefore leave the subdomain on which $u_2 \sim J$ is small and enter the subdomain where $u_2 \gg J$. Similarly when $u_1$ is close to 1, solutions transitions from $u_3 < .6$ to $u_3 > .6$, and the sign of the first entry of $(0.6 - u_3, 0.4 - u_1, 0.3 - u_2)$ changes from positive to negative. Hence the first coordinate of the solution starts decreasing (see Fig. 6, panel (f)), and solutions leave the subdomain where $1 - u_1 \sim J$ and enter another where $1 - u_1 \gg J$.

The BN corresponding to Eq. (10), $h = (h_1, h_2, h_3) : \{0, 1\}^3 \to \{0, 1\}^3$, is given by $h(x) = H(0.6 - x_3, 0.4 - x_1, 0.3 - x_2)$, where $H$ is the Heaviside function acting entry-wise on the arguments. Eq. (10) does not have steady states at the corner subdomains, and neither does the corresponding BN. A subset of states belong to a periodic orbit of the BN:

$$(0, 1, 1) \to (0, 1, 0) \to (1, 1, 0) \to (1, 0, 0) \to (1, 0, 1) \to (0, 0, 1) \to (0, 1, 1).$$

Note that adjacent states in this orbit differ in a single entry. Thus, the transitions between the states have an unambiguous interpretation in the original system: The BN predicts that if the initial condition is in chamber $\mathscr{C}^3_{12}$, then solutions of Eq. (10) will go to chamber $\mathscr{C}^{23}_1$, then to $\mathscr{C}^2_{13}$, and so on. Indeed, solutions of Eq. (10), are attracted to a periodic orbit that transitions between the chambers in this order. The remaining two states form a period two orbit under synchronous update, (1, 1, 1) ↔ (0, 0, 0); here the BN does not give precise information about the dynamics of the original system. We will show that under certain conditions, orbits of the BN where only entry changes at each timestep, correspond to oscillations in the original system.

## 3 General reduction of the model system

The approximations described in the previous section can be extended to the more general model in Eq. (1):

$$\frac{du_1}{dt} = A_i \frac{1 - u_i}{J + 1 - u_i} - I_i \frac{u_i}{J + u_i},$$

where $J > 0$ and $A_i$ and $I_i$ are activation/inhibition functions that capture the impact of other variables on the evolution of $u_i$. The initial conditions are assumed to satisfy $u_i(0) \in [0, 1]$ for all $i$.

We assume that the activation and inhibition functions are both affine and nonnegative [Novak et al. (2001); De Jong (2002)],

$$A_i := \sum_{j=1}^{N} w_{ij}^{+} u_j + b_i^{+}, \quad I_i := \sum_{j=1}^{N} w_{ij}^{-} u_j + b_i^{-}, \quad (11)$$

where we use the convention $x^+ = \max\{x, 0\}$ and $x^- = \max\{-x, 0\}$. The $N \times N$ matrix, $W = [w_{ij}]$ and the $N \times 1$ vector $b = [b_1\ b_2\ \ldots\ b_N]^t$ capture the connectivity and external input to the network, respectively. In particular, $w_{ij}$ gives the contribution of the $j^{\text{th}}$ variable to the growth rate of $i^{\text{th}}$ variable. If $w_{ij} > 0$, then $w_{ij}$ appears in the activation function for $u_i$; and if $w_{ij} < 0$ then $-w_{ij}$ appears in the inhibition function for $u_i$. The intensity of the external input to the $i^{\text{th}}$ element is $|b_i|$, and it contributes to the activation or the inhibition function, depending on whether $b_i > 0$ or $b_i < 0$, respectively.

**Proposition 1—**The cube $[0, 1]^N$ is invariant for Eq. (1).

**Proof:** It will be enough to show that the vector field at any point on the boundary is not directed outward. Since, $A_i \geq 0$ and $I_i \geq 0$, for any $i$,

$$\frac{du_i}{dt}\Big|_{u_i=0} = A_i \frac{1}{J+1} \geq 0, \quad \text{and} \quad \frac{du_i}{dt}\Big|_{u_i=1} = -I_i \frac{1}{J+1} \leq 0 \ .$$

□

### 3.1 The PL approximation

To obtain a solvable reduction of Eq. (1) we follow the procedure outlined in Section 2. We first present the results, and provide the mathematical justification in the next section. We will use $\delta = \delta(J) > 0$ to define the thickness of the boundary layers. We start with the subdivision of the $N$-dimensional cube, $[0, 1]^N$.

Let $T$ and $S$ be two disjoint subsets of $\{1, 2, \ldots, N\}$, and let

$$\mathscr{R}_S^T := \left\{ (u_1, u_2, \ldots, u_N) \in [0,1]^N \,|\, u_s < \delta \text{ for all } s \in S;\ u_t > 1-\delta \text{ for all } t \in T; \text{and } \delta \leq u_k \leq 1-\delta \text{ for all } k \notin S \cup T \right\}. \quad (12)$$

We extend the convention used in Table 1, and in Eqs. (3) and (5) so that $\mathscr{R}^T := \mathscr{R}_S^T$ when $S$ is empty; $\mathscr{R}_S := \mathscr{R}_S^T$ when $T$ is empty; and $\mathscr{R}_S := \mathscr{R}_S^T$ when $T$, $S$ are both empty.

Within each subdomain $\mathscr{R}_S^T$, Eq. (1) can be approximated by a different linear differential–algebraic system. Following the reduction from Eq. (2) to Eq. (6), for $i \notin S \cup T$ we obtain the linear system

$$\frac{du_i}{dt}=\sum_{j=1}^{N} w_{ij}u_j+b_i. \quad (13a)$$

For $s \in S$ one of the nonlinear terms remains and we obtain

$$\frac{du_s}{dt}=\left(\sum_{j=1}^{N} w_{sj}^{+}u_j+b_s^{+}\right)-\left(\sum_{j=1}^{N} w_{sj}^{-}u_j+b_s^{-}\right)\frac{u_s}{J+u_s}, \quad (13b)$$

while for $t \in T$ we will have

$$\frac{du_t}{dt}=\left(\sum_{j=1}^{N} w_{tj}^{+}u_j+b_t^{+}\right)\frac{1-u_t}{J+1-u_t}\left(\sum_{j=1}^{N} w_{tj}^{-}u_j+b_t^{-}\right). \quad (13c)$$

Eq. (13) is simpler than Eq. (1), but it is not solvable yet. Following the reduction from Eq. (6) to Eq. (7), we now further reduce Eqs. (13b–13c). First we use the approximations $u_s \approx 0$ and $u_t \approx 1$ in the activation and inhibition functions appearing in Eq. (13). Second, based on GSPT, we assume that $u_s$ for $s \in S$ and $u_t$ for $t \in T$ are in steady state.

Under these assumptions we obtain the reduction of Eq. (1) within any subdomain $\mathscr{R}_S^T$

$$\frac{du_i}{dt}=\sum_{j\notin S\cup T} w_{ij}u_j+\sum_{j\in T} w_{ij}+b_i \qquad i \notin S\cup T; \quad (14a)$$

$$0=\sum_{j\notin S\cup T} w_{sj}^{+}u_j+\sum_{j\in T} w_{sj}^{+}+b_s^{+}-\left(\sum_{j\notin S\cup T} w_{sj}^{-}u_j+\sum_{j\in T} w_{sj}^{-}+b_s^{-}\right)\frac{u_s}{J+u_s}, \qquad s \in S; \quad (14b)$$

$$0=-\left(\sum_{j\notin S\cup T} w_{tj}^{+}u_j+\sum_{j\in T} w_{tj}^{+}+b_t^{+}\right)\frac{1-u_t}{J+1-u_t}+\sum_{j\notin S\cup T} w_{tj}^{-}u_j+\sum_{j\in T} w_{tj}^{-}+b_t^{-}, \qquad t \in T. \quad (14c)$$

Eq. (14) is solvable since Eq. (14a) is decoupled, and Eqs.(14b) and (14c) are solvable for $u_s$ and $u_t$, respectively, as functions of the solution of Eq. (14a).

We remark that whenever one of the algebraic equations in Eq. (14) does not have a solution in a subdomain, the corresponding coordinate, say $u_j$, will jump from the interior of the subdomain ($u_j \approx 0$ or $u_j \approx 1$) to the adjacent subdomain ($u_j \gg 0$ or $1 - u_j \gg 0$).

Note that in the singular limit $J = 0$ the subdomains become corners, edges, faces, etc., and we obtain the 0-th order approximations:

$$\begin{aligned}\frac{du_i}{dt} &= \sum_{j\notin S\cup T} w_{ij}u_j + \sum_{j\in T} w_{ij} + b_i \qquad i \notin S\cup T;\\ u_s &= 0, \qquad s\in S;\\ u_t &= 1, \qquad t\in T.\end{aligned}$$

Alternatively, since as $J \to 0$ the interior region $\mathscr{R}$ approaches $(0, 1)^N$, it follows that the 0-th order approximation can also be written as a linear system with the additional condition that solutions must remain in [0, 1]. Then, it follows that the closed form expression of the 0-th order approximation is

$$\frac{du_i}{dt} = P\left(\sum_{j=1}^{N} w_{ij}u_j + b_i, u_i\right), \quad (16)$$

where $P$ is defined as

$$P(\lambda,\beta) = \begin{cases} \lambda & \text{if } \beta \in (0,1),\\ \lambda^+ & \text{if } \beta \le 0,\\ \lambda^- & \text{if } \beta \ge 1.\end{cases}$$

We remark that for models that are constructed using Hill functions, in the limit $n \to \infty$ the vector field becomes an algebraic combination of Heaviside functions. Analogously in our framework, in the limit $J \to 0$ the vector field becomes the "truncated" linear system given by Eq. (16). Thus, Eq. (16) can be seen as the $J = 0$ version of the classic piecewise linear systems that are constructed by combining Hill functions. Note that although Eq. (16) defines an ODE with discontinuous vector field, the solutions are continuous because the discontinuities in the vector field only force the system to remain in $[0, 1]^N$ and allows sliding on the boundary of $[0, 1]^N$. Also, note that to construct the 0-th order approximation it is enough to know the matrix $W$ and the vector $b$.

### 3.2 Boolean approximation

To obtain the Boolean approximation we follow the process described in Section 2. We consider the chambers determined by the complement of the union of the $N$ hyperplanes $\sum_{j=1}^{N} w_{ij}u_j + b_i = 0$ (restricted to $[0, 1]^N$) where $i = 1, \ldots, N$. We denote this set of hyperplanes by $\mathscr{H}$ and denote with $\Omega$ the set of all chambers $\Omega := \{\mathscr{C} : \mathscr{C} \text{ is a chamber}\}$; alternatively $\Omega$ is the set of connected components of $[0,1]^N \setminus \cup_{i=1}^{N} \{u : \sum_{j=1}^{N} w_{ij}u_j + b_i = 0\}$. We assume that $\mathscr{C}_S^T$ for all $i = 1, \ldots, N$ and for all $x \in \{0, 1\}^N$. This guarantees that each corner of $[0, 1]^N$ belongs to a chamber. The set of parameters excluded by this assumption has measure zero.

Let $S$ and $T$ be two disjoint subsets of $\{1, 2, \ldots, N\}$ such that $S \cup T = \{1, 2, \ldots, N\}$ and let $x \in \{0, 1\}^N$ be the corner that belongs to the corner subdomain $\mathscr{R}_S^T$. Note that $x_i = 0$ for $i \in S$

and $x_i = 1$ for $i \in T$. The chamber $\mathscr{C} \in \Omega$ that contains the corner in subdomain $\mathscr{R}_S^T$ will be denoted by $\mathscr{C}_S^T$. We do not name the remaining chambers.

In general, the chambers can be more complex than in the examples of Section 2. Chambers do not have to be hypercubes, different corners may belong to the same chamber, and some chambers may not even contain a corner of $[0, 1]^N$, as illustrated in Fig. 7. In the first example, (0, 1) and (1, 1) belong to the same chamber, that is, $\mathscr{C}_1^2 = \mathscr{C}^{12}$, and neither $\mathscr{C}_{12}$ containing (0, 0), nor $\mathscr{C}_2^1$ containing (1, 0) are rectangles. Also, $\Omega$ has three elements: $\mathscr{C}_{12}$, $\mathscr{C}_2^1$, and $\mathscr{C}_2^1 = \mathscr{C}^{12}$. In the second example, two chambers do not contain any corner of $[0, 1]^2$ and are not named. Hence, $\Omega$ has four elements: $\mathscr{C}_{12} = \mathscr{C}_1^2$, $\mathscr{C}_2^1 = \mathscr{C}^{12}$, and two unnamed chambers that contain no corners.

To define the BN, $h = (h_1, \ldots, h_N) : \{0, 1\}^N \to \{0, 1\}^N$ at $x \in \{0, 1\}^N$, we need to find the signs of the components of the vector field $Wu + b$ on the chamber that contains $x$. Consider $x \in \mathscr{R}_S^T$. Within $\mathscr{C}_S^T$ the signs of the components of $Wu + b$ do not change and are equal to the signs of the components of $Wx + b$. If the sign of the $i$-th component is negative, we let $h_i(x) = 0$, and if the sign is positive we let $h_i(x) = 1$. In general, we can write

$$h_i(x) = H\left(\sum_{j=1}^{N} w_{ij}x_j + b_i\right), \quad \text{or in vector form} \quad h(x) = H(Wx + b). \tag{17}$$

Hence the value of the BN at a corner $x \in \mathscr{R}_S^T$ is given by the Heaviside function, applied entry-wise to $Wu + b$. Note that corners that are in the same chamber get mapped to the same point.

Importantly, using Eq. (17) we can compute the BN directly from Eq. (1). For example, for Eq. (2) we have $h(x_1, x_2) = H(0.5 - x_2, 0.5 - x_1)$; and for Eq. (10) we have $h(x_1, x_2, x_3) = H(0.6 - x_3, 0.4 - x_1, 0.3 - x_2)$.

Below we show that up to a set of small measure, the BN preserves information about the steady states of the original system. We will also show that under some conditions, “regular” trajectories of a BN correspond to trajectories in the original system.

## 4 Mathematical justification

We next justify the different approximations made above: In Section 4.1 we use Geometric Singular Perturbation Theory (GSPT) to justify the PL approximation. In Section 4.2 we show that steady state information is preserved by the BN and that, under certain conditions, the BN also provides qualitative information about the global dynamics of the original system.

### 4.1 Piecewise linear approximation

To obtain the reduced equations at the boundary of $[0, 1]^N$, we define the following rescaled variables

$$\tilde{u}_s := \frac{u_s}{J} \quad \text{for } s \in S, \text{ and } \quad \tilde{u}_t := \frac{1-u_t}{J} \quad \text{for } t \in T. \tag{18}$$

Using Eq. (18) in Eq. (13) we get for $i \notin S \cup T$

$$\frac{du_i}{dt} = \sum_{j \notin S \cup T} w_{ij} u_j + \sum_{j \in T} w_{ij} + J \left( \sum_{j \in S} w_{ij} \tilde{u}_j - \sum_{j \in T} w_{ij} \tilde{u}_j \right) + b_i, \tag{19a}$$

and for $s \in S$,

$$\begin{aligned} J \frac{d\tilde{u}_s}{dt} = & \sum_{j \notin S \cup T} w_{sj}^+ u_j + \sum_{j \in T} w_{sj}^+ + J \left( \sum_{j \in S} w_{sj}^+ \tilde{u}_j - \sum_{j \in T} w_{sj}^+ \tilde{u}_j \right) + b_s^+ \\ & - \left( \sum_{j \notin S \cup T} w_{sj}^- u_j + \sum_{j \in T} w_{sj}^- + b_s^- \right) \frac{\tilde{u}_s}{1+\tilde{u}_s} - J \left( \sum_{j \in S} w_{sj}^+ \tilde{u}_j - \sum_{j \in T} w_{sj}^+ \tilde{u}_j \right) \frac{\tilde{u}}{1+\tilde{u}_s}, \end{aligned} \tag{19b}$$

and similarly, for $t \in T$,

$$\begin{aligned} J \frac{d\tilde{u}_t}{dt} = & - \left( \sum_{j \notin S \cup T} w_{tj}^+ u_j + \sum_{j \in T} w_{tj}^+ + b_t^+ \right) \frac{\tilde{u}_t}{1+\tilde{u}_t} - J \left( \sum_{j \in S} w_{tj}^+ \tilde{u}_j - \sum_{j \in T} w_{tj}^+ \tilde{u}_j \right) \frac{\tilde{u}_t}{1+\tilde{u}_t} \\ & + \sum_{j \notin S \cup T} w_{tj}^- u_j + \sum_{j \in T} w_{tj}^- + b_t^- + J \left( \sum_{j \in S} w_{tj}^+ \tilde{u}_j - \sum_{j \in T} w_{tj}^+ \tilde{u}_j \right). \end{aligned} \tag{19c}$$

When $J$ is small, we can apply Geometric Singular Perturbation Theory (GSPT) to Eq. (19) [Hek (2010); Kaper (1998)]. The GSPT posits that, under a normal hyperbolicity condition which we verify below, Eq. (19) can be further simplified by assuming that $J = 0$. This yields a differential-algebraic system

$$\frac{du_i}{dt} = \sum_{j \notin S \cup T} w_{ij} u_j + \sum_{j \in T} w_{ij} + b_i, \qquad i \notin S \cup T; \tag{20a}$$

$$0 = \sum_{j \notin S \cup T} w_{sj}^+ u_j + \sum_{j \in T} w_{sj}^+ + b_s^+ - \left( \sum_{j \notin S \cup T} w_{sj}^- u_j + \sum_{j \in T} w_{sj}^- + b_s^- \right) \frac{\tilde{u}_s}{1+\tilde{u}_s}, \qquad s \in S; \tag{20b}$$

$$0 = - \left( \sum_{j \notin S \cup T} w_{tj}^+ u_j + \sum_{j \in T} w_{tj}^+ + b_t^+ \right) \frac{\tilde{u}_t}{1+\tilde{u}_t} + \sum_{j \notin S \cup T} w_{tj}^- u_j + \sum_{j \in T} w_{tj}^- + b_t^-, \qquad t \in T. \tag{20c}$$

which is equivalent to Eq. (14) after rescaling. This conclusion is justified if the manifold defined by Eqs. (20b) and (20c) is normally hyperbolic and stable [Fenichel (1979); Kaper (1998); Hek (2010)]. We verify this condition next.

Let $\hat{u} = \{u_j : j \notin S \cup T\}$, be the coordinates of $u$ which are away from the boundary, and denote the right hand side of Eq. (20b) by $F_s(\hat{u}, \tilde{u}_s)$, for all $s \in S$, so that

$$F_s(\hat{u},\tilde{u}_s):=\sum_{j\notin S\cup T} w_{sj}^{+}u_j+\sum_{j\in T} w_{sj}^{+}+b_s^{+}-\left(\sum_{j\notin S\cup T} w_{sj}^{-}u_j+\sum_{j\in T} w_{sj}^{-}+b_s^{-}\right)\frac{\tilde{u}_s}{1+\tilde{u}_s},$$

and

$$\frac{\partial F_s}{\partial \tilde{u}_s}=-\left(\sum_{j\notin S\cup T} w_{sj}^{-}u_j+\sum_{j\in T} w_{sj}^{-}+b_s^{-}\right)\left(\frac{1}{1+\tilde{u}_s}\right)^2<0,$$

for all $s \in S$. Similarly, by denoting the right hand side of Eq. (20c) by $G_t(\hat{u}, \tilde{u}_t)$, for all $t \in T$. *i.e.*

$$G_t(\hat{u},\tilde{u}_t):=-\left(\sum_{j\notin S\cup T} w_{tj}^{+}u_j+\sum_{j\in T} w_{tj}^{+}+b_t^{+}\right)\frac{\tilde{u}_t}{1+\tilde{u}_t}+\sum_{j\notin S\cup T} w_{tj}^{-}u_j+\sum_{j\in T} w_{tj}^{-}+b_t^{-},$$

we see that

$$\frac{\partial G_t}{\partial \tilde{u}_t}=-\left(\sum_{j\notin S\cup T} w_{tj}^{+}u_j+\sum_{j\in T} w_{tj}^{+}+b_t^{+}\right)\left(\frac{\tilde{u}_t}{1+\tilde{u}_t}\right)^2<0.$$

Hence, the manifold defined by Eqs. (20b) and (20c) is normally hyperbolic and stable. This completes the proof that the reduction of the non-linear system (1) to the solvable system given in Eq. (14) is justified for small $J$.

### 4.2 Boolean approximation

Here we show that the steady states of the BN given in Eq. (17) are in a one-to-one correspondence with the steady states of the system given in Eq. (1). We also show that under some conditions trajectories in the BN correspond to trajectories of the system given in Eq. (1).

**4.2.1 Steady state equivalence at the corner subdomains—**First we prove the one-to-one correspondence only at the corner subdomains using the PL approximation. We do this by showing that Eq. (14) has a steady state at a corner subdomain $\mathscr{R}_S^T$ if and only if the BN has a steady state at the corner $x \in \{0, 1\}^N$ contained in $\mathscr{R}_S^T$.

We proceed from Eq. (14) for a corner subdomain $\mathscr{R}_S^T$ so that $S \cup T = \{1, \ldots, N\}$. We obtain the equations

$$0=\sum_{j\in T} w_{sj}^{+}+b_s^{+}-\left(\sum_{j\in T} w_{sj}^{-}+b_s^{-}\right)\frac{u_s}{J+u_s},\quad s\in S$$

and

$$0=-\left(\sum_{j\in T}w_{tj}^{+}+b_t^{+}\right)\frac{1-u_t}{J+1-u_t}+\sum_{j\in T}w_{tj}^{-}+b_t^{-},\quad t\in T.$$

For the sets $S$ and $T$, consider $x\in\{0,1\}^N$ such that $x_s=0$ for all $s\in S$ and $x_t=1$ for all $t\in T$. Then, since $\sum_{j\in T}w_{sj}^{+}=\sum_j w_{sj}^{+}x_j$, $\sum_{j\in T}w_{sj}^{-}=\sum_j w_{sj}^{-}x_j$, $\sum_{j\in T}w_{tj}^{+}=\sum_j w_{tj}^{+}x_j$, and $\sum_{j\in T}w_{tj}^{-}=\sum_j w_{tj}^{-}x_j$, we can write the equations above in the form

$$0=\sum_{j=1}^{N}w_{sj}^{+}x_j+b_s^{+}-\left(\sum_{j=1}^{N}w_{sj}^{-}x_j+b_s^{-}\right)\frac{u_s}{J+u_s},\quad s\in S$$

and

$$0=-\left(\sum_{j=1}^{N}w_{tj}^{+}x_j+b_t^{+}\right)\frac{1-u_t}{J+1-u_t}+\sum_{j=1}^{N}w_{tj}^{-}x_j+b_t^{-},\quad t\in T,$$

or in the more compact form

$$0=A_s(x)-I_s(x)\frac{u_s}{J+u_s},\quad s\in S$$

and

$$0=-A_t(x)\frac{1-u_t}{J+1-u_t}+I_t(x),\quad t\in T.$$

Solving these equations for $u_s$ and $u_t$, respectively, we obtain

$$u_s=-\frac{A_s(x)J}{A_s(x)-I_s(x)},\quad s\in S,\quad\text{and},\quad u_t=1-\frac{I_t(x)J}{A_t(x)-I_t(x)},\quad t\in T.\quad(21)$$

Now, let $\in>0$ be sufficiently small so that $\left|\frac{I_s(x)J}{A_s(x)-I_s(x)}\right|,\left|\frac{I_t(x)J}{A_t(x)-I_t(x)}\right|\leq 1$ for all $0<J<\in$. Then, for all $J$ such that $0<J<\in$, Eq. (21) has a solution inside $[0,1]^N$ if and only if

$$A_s(x)-I_s(x)<0, s\in S\quad\text{and},\quad A_t(x)-I_t(x)>0, t\in T,$$

or equivalent if and only if

$$H(A_s(x)-I_s(x))=0, s\in S\quad\text{and},\quad H(A_t(x)-I_t(x))=1, t\in T,$$

which can be written more compactly as

$$H(A_i(x) - I_i(x)) = x_i \text{ for all } i = 1, \ldots, N.$$

Thus, a steady state appears in the corner subdomain corresponding to $x$ if and only if $x$ is a steady state of the BN $h = (h_1, \ldots, h_N) : \{0,1\}^N \to \{0,1\}^N$ given by Eq. (17). We have proved,

**Theorem 2:** There is an $\epsilon > 0$ such that for all $0 < J < \epsilon$, Eq. (14) has a steady state at a corner subdomain containing $x \in \{0,1\}^N$ if and only if the BN described by Eq. (17) has a steady state at $x$.

Since the PL system given by Eq. (14) is a valid approximation of the full system given in Eq. (1) (guaranteed by GSPT as shown in Section 4.1), we also have the following corollary.

**Corollary 3:** There is an $\epsilon > 0$ such that for all $0 < J < \epsilon$, the system in Eq. (1) has a steady state at a corner subdomain containing $x \in \{0,1\}^N$ if and only if the BN in Eq. (17) has a steady state at $x$.

**4.2.2 Global equivalence of steady states—**We proved that, for $J$ small, the steady states at the corner subdomains of the system in Eq. (1) are in a one-to-one correspondence with the steady states of the BN. However, the corner subdomains only cover a small portion of $[0,1]^N$. We next show that the steady state correspondence is global (thus, generalizing Corollary 3).

Recall that $\Omega = \{\mathscr{C} : \mathscr{C} \text{ is a chamber}\}$ and that each chamber is a connected component of $[0,1]^N \setminus \cup_{i=1}^N \{u : \sum_{j=1}^N w_{ij} u_j + b_i = 0\}$. The chambers are bounded convex open subsets of $[0,1]^N$ (with the topology inherited from $[0,1]^N \subset R^N$). Also note that $[0,1]^N \setminus \cup_{\mathscr{C} \in \Omega} \mathscr{C}$ is the union of the hyperplanes in $\mathscr{H}$ and hence has measure zero. We denote by $\mathscr{C}(x)$ the chamber that contains the point $x \in [0,1]^N$.

**Theorem 4:** Let $K$ be a compact subset of $\cup_{\mathscr{C} E \Omega} \mathscr{C}$ such that $K \cap \mathscr{C}$ is convex for any $\mathscr{C} \in \Omega$, and such that $K \cap \mathscr{C}(x)$ contains a neighborhood of $x$ for each $x \in \{0,1\}^N$.

Then, there is an $\epsilon_K > 0$ such that for all $0 < J < \epsilon_K$, if $x^* \in \{0,1\}^N$ is a steady state of the BN in Eq. (17), then the ODE in Eq. (1) has a steady state $u^* \in \mathscr{C}(x^*)$; also, if $u^* \in K$ is a steady state of the ODE, then $u^* \in \mathscr{C}(x^*)$ for some steady state $x^*$ of the BN.

Furthermore, if $x^*$ is a steady state of the BN in Eq. (17), then the steady state of the ODE in Eq. (1) is unique in $K \cap \mathscr{C}(x^*)$, converges to $x^*$ as $J \to 0$, and is asymptotically stable.

***Proof:*** See Appendix. □

We can make the set $K$ in Theorem 4 as close to $[0,1]^N$ as desired. For example, for each chamber $\mathscr{C}$ and for $r > 0$, denote $K_{\mathscr{C}} := \{u \in \mathscr{C} : |\sum_{j=1}^{N} w_{ij}u_j + b_i| \geq r, \forall i\}$. By using $r$ small, and denoting Lebesgue measure by $\mu$, we can make $\mu([0,1]^N \setminus \cup_{\mathscr{C}\in\Omega} K_{\mathscr{C}}) = \mu(\cup_{\mathscr{C}\in\Omega}(\mathscr{C}\setminus K_{\mathscr{C}})) = \sum_{\mathscr{C}\in\Omega} \mu(\mathscr{C}\setminus K_{\mathscr{C}})$ as small as desired. Hence, we have the following corollary.

**Corollary 5:** For any $\epsilon > 0$, there is a set $K \subseteq [0,1]^N$ satisfying $\mu([0,1]^N \setminus K) < \epsilon$ and a number $\epsilon_K$ such that for all $0 < J < \epsilon_K$, there is a one-to-one correspondence between the steady states of the BN in Eq. (17) and the steady states in $K$ of the ODE in Eq. (1). Furthermore, the steady states of the ODE in $K$ are asymptotically stable.

Note that the set $K$ does not include the nullclines. Hence, steady states outside $K$ are possible, and they could be stable. Such steady states can be studied using the PL approximation in Eq. (14a).

**4.2.3 Equivalence of trajectories—**We next examine under which conditions the trajectories of the BN in Eq. (17) correspond trajectories of the ODE given in Eq. (1). The main assumption in the rest of this section is that the hyperplanes in $\mathscr{H}$ divide $[0,1]^N$ into $2^N$ chambers, and that each chamber contains a corner.

We say that the solutions of the system in Eq. (1) *transition from* $K \subseteq [0,1]^N$ *to* $K' \subseteq [0,1]^N$ if for any solution of the system, $u(t)$, with initial condition $u(0) \in K$, there exists $\hat{t}$ such that $u(\hat{t}) \in K'$. The *Hamming distance* between $x, y \in \{0,1\}^N$ is defined as the number of entries where $x$ and $y$ differ; that is, $d(x, y) := \#\{i \in \{1, \ldots, N\} : x_i \neq y_i\}$. We denote a transition $h(x) = y$ (i.e. $H(Wx + b) = y$) with $x \to y$. A trajectory is a sequence of transitions and is denoted similarly. We call a transition $x \to y$ *regular* if either (1) $x = y$ or (2) $d(x, y) = 1$ and $h_j(y) = y_j$ for the index $j$ for which $x_i \neq y_i$. In other words, a transition $x \to y$ in the BN is regular if $x$ is a steady state or if $x$ transitions to $y$ by changing only one coordinate and this coordinate does not change back when transitioning from $y$ to $h(y)$. For example, if $000 \to 100 \to 111$, then $000 \to 100$ is a regular transition ($j = 1$); on the other hand, if $000 \to 100 \to 010$, then $000 \to 100$ is not a regular transition. A trajectory is regular if each component transition is regular.

**Theorem 6:** Suppose that the hyperplanes in $\mathscr{H}$ divide $[0,1]^N$ into $2^N$ chambers and consider a regular transition of the BN in Eq. (17), $x \to h(s)$. Then, there is a neighborhood $K$ of $x$, and an $\epsilon_K > 0$ such that for all $0 < J < \epsilon_K$ the solutions of the ODE in Eq. (1) transition from $K$ to $\mathscr{C}(h(x))$. Also, if $x$ is a steady state, the neighborhood $K$ can be chosen to be invariant.

***Proof:*** See Appendix. □

Next for a steady state $x$ define $B_1(x) = \{y \in \{0, 1\}^N : h(y) = x \text{ and } d(x, y) \leq 1\}$; that is, $B_1(x)$ is the set of states in the basin of attraction of $x$ with Hamming distance at most 1 from $x$. The following corollary of Theorem 6 states that this part of the basin of attraction of $x$

corresponds to part of the basin of attraction of the steady state in the ODE in Eq. (1) corresponding to $x$.

**Corollary 7:** Suppose that $x$ is a steady state of the BN in Eq. (17). Then, for every $y \in B_1(x)$, there is a neighborhood $K$ of $y$ and $\epsilon_K > 0$, such that for all $0 < J < \epsilon_K$ the solutions of the ODE in Eq. (1) transition from $K$ to $\mathscr{C}(x)$.

Note that Theorem 6 implies that for a regular trajectory of the BN in Eq. (17), $x \to h(x) \to h^2(x) \to \ldots \to h^m(x)$, the solutions of the ODE in Eq. (1) will transition from a neighborhood of $x$ to $\mathscr{C}(h(x))$, from a neighborhood of $h(x)$ to $\mathscr{C}(h^2(x))$ and so on. To guarantee that a neighborhood of $x$ will reach a neighborhood of $h^m(x)$ (that is, to guarantee that the result is "transitive"), we need the additional assumption that each hyperplane in $\mathscr{H}$ is orthogonal to some coordinate axis. Note that the example given in Section 2.2 satisfies this condition.

**Theorem 8:** Suppose that each hyperplane in $\mathscr{H}$ is orthogonal to some coordinate axis and let $x \to h(x) \to \ldots \to h^m(x)$ be a regular trajectory of the BN in Eq. (17). Then, for any compact set $K \subset \mathscr{C}(x)$ there is $\epsilon_K > 0$ such that for all $0 < J < \epsilon_K$, the solutions of the ODE in Eq. (1) transition from $K$ to $\mathscr{C}(h^m(x))$ following the order of the regular trajectory.

***Proof:*** See Appendix. □

For a steady state of the BN define $B(x) = \{y$ : there is a regular trajectory from $y$ to $x\}$. The following corollary of Theorem 8 implies that some states in the basin of attraction of a steady state of the BN in Eq. (17) correspond to chambers in the basin of attraction of a steady state of the ODE in Eq. (1).

**Corollary 9:** Suppose that each hyperplane in $\mathscr{H}$ is orthogonal to some coordinate axis and let $x$ be a steady state of the BN in Eq. (17). Consider $y \in B(x)$. Then, for any compact set $K \subseteq \mathscr{C}(y)$, there exists $\epsilon_K > 0$ such that for all $0 < J < \epsilon_K$, the solutions of the ODE in Eq. (1) transition from $K$ to $\mathscr{C}(x)$.

Similarly, we obtain the following corollary for oscillatory behavior.

**Corollary 10:** Suppose that each hyperplane $\mathscr{H}$ is orthogonal to some coordinate axis and let $x^1 \to x^2 \to \ldots \to x^p \to x^1$ be a regular periodic orbit of the BN in Eq. (17). Then, for any compact set $K \subseteq \mathscr{C}(x^1)$ and any positive integer m, there exists $\epsilon_{K,m} > 0$ such that for all $0 < J < \epsilon_{K,m}$, the solutions of the ODE in Eq. (1) transition between the chambers (starting at $K$) in the order $\mathscr{C}(x^1), \mathscr{C}(x^2), \ldots, \mathscr{C}(x^p), \mathscr{C}(x^1)$, $m$ times.

Note that the example in Section 2.2 satisfies the hypothesis of this last corollary. In general, Corollary 10 does not guarantee that the solution is periodic.

Finally, we note that the requirement that there are $2^N$ chambers, each containing a corner is necessary. Even if we have a transition where only one variable changes (e.g. $h(1, 0) = (0, 0)$), having an intermediate chamber can change the behavior of the solutions before they reach the chamber predicted by the BN. In the example shown in Fig. 8 the signs of the

vector field of the approximating linear system imply that the BN transitions from (1, 0) to (0, 0). However, solutions can transition from the chamber that contains (1, 0) to the bottom middle chamber and never reach the chamber that contains (0, 0). In summary, even having a transition where only one variable changes may not be sufficient to guarantee that the Boolean transition corresponds to a similar transition in the original system.

## 5 Discussion

Models of biological systems are frequently nonlinear and difficult to analyze mathematically. In addition, accurate models frequently contain numerous parameters whose exact values are not known. Thus, studying which parameters have a large impact on dynamics, and how a model can be simplified, is crucial in finding the features of biological systems that determine their behavior and responses. Reduction techniques that preserve key dynamical properties are essential in this endeavor.

We studied a special class of non-linear differential equation models of biological networks where interactions between nodes are described using Hill functions. When the Michaelis-Menten constants are sufficiently small, the behavior of the system is captured by an approximate piecewise linear system and a Boolean Network. In this case the domain of the full system naturally decomposes into nested hypercubes. These hypercubes define subdomains within which a solvable linear–algebraic system approximates the original system. The Boolean Network is obtained from a decomposition of the domain into chambers and describes how solutions evolve between them.

The proposed reductions have a number of advantages: The piecewise linear approximation is not only easier to solve than the original system analytically, but also numerically (the original system becomes stiff for small $J$). Also, we have given the 0-th order approximation in closed form. When one is interested in qualitative behavior such as steady state analysis, the Boolean approximation can be very useful, especially when the dimension of the system is large. Also, the Boolean framework has been used to model many biological systems where it is assumed that interactions are switch-like and variables can be discretized. It is therefore important to know when, and in what sense such reduced systems can be justified, and in particular, what dynamical properties of the full system are captured by a reduction.

Although the case of large exponent $n$ in the Hill function has been studied in the past [Glass and Kauffman (1973); Glass (1975,b); Snoussi (1989); Thomas and D'Ari (1990); Mendoza and Xenarios (2006); Davidich and Bornholdt (2008); Wittmann et al. (2009); Franke (2010); Veliz-Cuba et al. (2012)], the case of small $J$ has been studied only recently and heuristically [Davidich and Bornholdt (2008)]. In this manuscript we have shown that the PL and the BN approximations are also valid for the case of small $J$, and have given explicit formulas for their computation. The BN approximation preserves steady state behavior and under further restrictions, it can also be used to infer the basins of attractions and oscillations in the original system. Note that the Boolean functions in the Boolean approximation are threshold functions, as used in earlier models [Li et al. (2004); Davidich and Bornholdt (2008b)]. Our results show that such BNs can indeed appear when approximating more detailed models, such as those described by Eq. (1). In summary, our results for the limit $J$

$\to 0$ complement previous results for the limit $n \to \infty$, providing a useful framework for reducing nonlinear systems to PL systems and BNs.

A potential limitation in our arguments is that we have an approximation valid only in an asymptotic limit. It is unknown when and how the approximation breaks down. However, the approximation is still valid as $J$ increases until we reach a bifurcation point, which can happen for relative large $J$ or for values of $J$ that are biologically relevant. Also, we have not provided a systematic relationship between the thickness of the boundary, $\delta$, and the Michaelis-Menten constant, $J$. Numerical tests suggest that the relationship is between $J = O(\delta)$ and $J = O(\delta^2)$. Another limitation of our analysis is that, in the general case, it is not known when the transitions or cycles in a BN will correspond to similar transitions or cycles in the original ODE.

Although the requirement of regularity may be restrictive, preliminary results indicate that our results hold under weaker requirements. However, the proofs seem to be much more technical. One such way to obtain a better agreement between the Boolean approximation and the original system is to use alternative update rules. For example, in the limit $n \to \infty$, using an asynchronous update rule can some times give a better match between the Boolean approximation and the continuous system [Glass and Kauffman (1973); Glass (1975,b); Thomas and D'Ari (1990); Snoussi (1989); Abou-Jaoudé et al. (2009)]. However, an asynchronous update rule produces non-deterministic dynamics and trajectories have to be carefully defined. Our results also show that Boolean reductions of ODEs have to be interpreted with care in general. The correspondence between the BN and ODE dynamics is often implicitly assumed and we have shown that in general such a correspondence only holds for steady states. For trajectories and periodic orbits the relationship will not always be valid, but our theory gives precise conditions under which this dynamical correspondence holds.

## Acknowledgments

We thank Matthew Bennett for help in preparing the manuscript. This work was funded by the NIH, through the joint NSF/NIGMS Mathematical Biology Program Grant No. R01GM104974.

# 6 Appendix

## 6.1 Motivation of Eq. (1)

Here we present a heuristic justification of the use of Eq. (1). The ideas follow those presented in [Goldbeter and Koshland (1981); Goldbeter (1991); Novak et al. (1998, 2001); Tyson et al. (2003); Aguda (2006)]. As mentioned in the Introduction, this is only heuristic in general.

Consider a protein that can exist in an unmodified form, $W$, and a modified form, $W^*$, where the conversion between the two forms is catalyzed by two enzymes, $E_1$ and $E_2$. That is, consider the reactions

$$W+E_1 \underset{k_{-1}}{\overset{k_1}{\rightleftarrows}} WE_1 \xrightarrow{p_1} W^*+E_1,$$
$$W^*+E_2 \underset{k_{-2}}{\overset{k_2}{\rightleftarrows}} W^*E_2 \xrightarrow{p_2} W+E_2.$$

Then, using quasi-steady-state assumptions one can obtain the equation

$$\frac{dW^*}{dt}=A\frac{L-W^*}{K_1+L-W^*}-I\frac{W^*}{K_2+W*},$$

where $A$, $I$, $L$, $K_1$, $K_2$ depend on $k_1$, $k_{-1}$, $p_1$, $k_2$, $k_{-2}$, $p_2$, $[E_1]$, $[WE_1]$, $[E_2]$, and $[W^*E_2]$ [Goldbeter and Koshland (1981)]. After rescaling by $L$ we obtain Eq. (1).

Now, consider a system with $N$ species (e.g. proteins) and assume that $u_i(t)$ and $v_i(t)$ represent the concentration of species $i$ at time $t$ in its active and inactive form, respectively. Furthermore, suppose that the total concentration of each species is constant and that the difference between decay and production is negligible (so that $u_i(t) + v_i(t)$ is constant). That is,

$$u_i(t)+v_i(t)=L_i,$$

where $L_i$ does not depend on time, and

$$\frac{du_i}{dt}=\text{rate of activation}-\text{rate of inhibition}.$$

Then, using Michaelis-Menten kinetics, the rate of activation of this species can be modeled by

$$\text{rate of activation}=A_i\frac{v_i}{K_i^A+v_i}=A_i\frac{L_i-u_i}{K_i^A+L_i-u_i},$$

where the maximal rate, $A_i = A_i(u)$, is a function of the different species in the network. Similarly, modeling the inhibition of the species using Michaelis-Menten kinetics, we obtain

$$\text{rate of inhibition}=I_i\frac{u_i}{K_i^I+u_i}.$$

Thus, we obtain

$$\frac{du_i}{dt}=A_i\frac{L_i-u_i}{K_i^A+L_i-u_i}-I_i\frac{u_i}{K_i^I+u_i}.$$

Now, we rescale $u_i \to L_iu_i$, $A_i \to L_iA_i$, $I_i \to L_iI_i$ and obtain

$$\frac{du_i}{dt}=A_i\frac{1-u_i}{\frac{K_i^A}{L_i}+1-u_i}-I_i\frac{u_i}{\frac{K_i^I}{L_i}+u_i}.$$

Hence, by denoting $J_i^A:=\frac{K_i^A}{L_i}$ and $J_i^I:=\frac{K_i^I}{L_i}$, we obtain the system given in Eq. (1). Also, $J_i^A$ and $J_i^I$ small means that the dissociation constants $(K_i^A, K_i^I)$ are much smaller than the total concentration of species *i*; that is, $J_i^A, J_i^I \ll 1$ if and only if $K_i^A, K_i^I \ll L_i$. Note that the initial conditions now satisfy $u_i(0) \in [0,1]$ for all *i*.

## 6.2 Behavior of $A\frac{1-x}{J+1-x}-I\frac{x}{J+x}$ as $J \to 0$

Consider the one-dimensional system

$$\frac{dx}{dt}=A\frac{1-x}{J+1-x}-I\frac{x}{J+x}. \quad (22)$$

Fig. 9 shows the graph of the right hand side of Eq. (22) for the fixed values $A = 1$, $I = 0.5$ and three different values of *J*. Note that as *J* becomes smaller, the graph gets flatter in (0,1). Then, for *J* small, we can approximate Eq. (22) in the interior of the region [0,1] by the linear ODE

$$\frac{dx}{dt}=A-I.$$

For $x \sim J$, we can approximate Eq. (22) by the ODE

$$\frac{dx}{dt}=A-I\frac{x}{J+x}.$$

And for $x \sim 1 - J$, we can approximate Eq. (22) by the ODE

$$\frac{dx}{dt}=A\frac{1-x}{J+1-x}-I.$$

For the values $A = 1$, $I = 0.5$ we obtain the following approximations.

$$\begin{array}{c}\frac{dx}{dt}=0.5, \text{ if } J \ll x \ll 1-J\\ \frac{dx}{dt}=1-0.5\frac{x}{J+x}, \text{ if } x\sim J\\ \frac{dx}{dt}=\frac{1-x}{J+1-x}-0.5, \text{ if } x\sim 1-J\end{array}$$

Note that there is an asymptotically stable steady state close to 1. Intuitively, for *J* small, solutions that start in the region $x \sim J$ quickly reach the region $J \ll x \ll 1$, which behaves

like a linear system. Then, solutions increase almost linearly (with slope 0.5) until they enter the region $x \sim 1 - J$ where they will approach the steady state (see Fig. 10).

We see that in the limit $J \to 0$ we obtain the solutions

$$x(t)=x(0)+0.5t \text{ for } t \in \left[0, \frac{1-x(0)}{0.5}\right] \text{ and } x(t)=1 \text{ for } t \in \left[\frac{1-x(0)}{0.5}, \infty\right),$$

where $x(0) \in [0, 1]$. Note that these functions are the solutions of the ODE

$$\frac{dx}{dt}=P(A-I,x)$$

given in Eq. (16) (0-th order approximation).

## 6.3 Proof of Theorem 4

The main idea in the proof is to use the fact that for $u_i \neq 0, 1$, the right-hand side of Eq. (1) converges to $Wu + b$. More precisely, the convergence is uniform on compact subsets of $(0, 1)^N$; so that we have compact convergence.

Also, given a steady state of Eq. (1), we can solve for $u_i$ and obtain $u_i=\Gamma_i^J(u)$ ( $\Gamma_i^J$ will be defined later). The proofs also use the fact that as $J \to 0$, $\Gamma^J=\left(\Gamma_i^J,\ldots,\Gamma_N^J\right)$ converges uniformly to the function $u \mapsto H(Wu+b)$ on compact subsets of each chamber. That is, we also have compact convergence of $\Gamma^J$.

To prove Theorem 4 we need the following definitions and lemmas.

A point $u^* \in [0, 1]^N$ will be a steady state of the ODE in Eq. (1) if and only if

$$A_i(u^*)\frac{1-u_i^*}{J+1-u_i^*} - I_i(u^*)\frac{u_i^*}{J+u_i^*}=0 \quad (23)$$

for all $i$. Solving the corresponding quadratic equation for $u_i^*$ we obtain the solutions $u_i^*=1/2$ if $A_i(u^*) = I_i(u^*)$; and

$$u_i^*=\frac{(A_i(u^*)-I_i(u^*)-A_i(u^*)J-I_i(u^*)J) \pm \sqrt{\Delta_i(u^*)}}{2(A_i(u^*)-I_i(u^*))} \quad (24)$$

if $A_i(u^*) \neq I_i(u^*)$, where $\Delta_i(u^*)$ is the discriminant of the quadratic equation, given by

$$\Delta_i(u):=(A_i(u)-I_i(u)-A_i(u)J-I_i(u)J)^2+4A_i(u)J(A_i(u)-I_i(u)).$$

The following lemma states that up to a set of small measure and for $J$ small all steady states of the ODE in Eq. (1) are given by the fixed points of the function $\Gamma^J=(\Gamma_1^J,\ldots,\Gamma_N^J)$ defined by

$$\Gamma_i^J(u) := \frac{(A_i(u) - I_i(u) - A_i(u)J - I_i(u)J) + \sqrt{\Delta_i(u)}}{2(A_i(u) - I_i(u))}. \quad (25)$$

**Lemma 11**

For any compact subset $K$ of $\cup_{\mathscr{C}\in\Omega}\mathscr{C}$, there is an $\in_K > 0$ such that for all $0 < J < \in_K$ the function $\Gamma^J$ is well-defined (as a real-valued function) on $K$, and $u^*$ is a steady state in $K$ of the ODE in Eq. (1) if and only if $\Gamma^J(u^*) = u^*$.

**Proof—**Since the denominator is not 0 on $K$, we need to show that $\Delta_i(u)$ is non negative on $K$ for $J$ small.

Since $K$ is compact and $A_i(u) - I_i(u) = \sum_{j=1}^N w_{ij}u_j + b_i \neq 0$ for all $i = 1, \ldots, N$ and for all $u \in K$, there is $r > 0$ such that $|A_i(u) - I_i(u)| = |\sum_{j=1}^N w_{ij}u_j + b_i| \geq r$ on $K$. Then, since $(A_i(u) - I_i(u) - A_i(u)J - I_i(u)J)^2 + 4A_i(u)J(A_i(u) - I_i(u))$ converges uniformly as $J \to 0$ to $(A_i(u) - I_i(u))^2 \geq r^2$ on K, there is $\in_K > 0$ such that for all $0 < J < \in_K$ the function $(A_i(u) - I_i(u) - A_i(u)J - I_i(u)J)^2 + 4A_i(u)J(A_i(u) - I_i(u))$ is positive on $K$ for all $i$. Thus, $\Gamma^J$ is well-defined for all $0 < J < \in_K$.

If $u^* \in K$ and $\Gamma^J(u^*) = u^*$, then $u^*$ satisfies Eq. (24), and hence it is a steady state of the ODE in Eq. (1). Also, if $u^*$ is a steady state of the ODE in Eq. (1), then $u^*$ satisfies Eq. (24). However, only $\Gamma_i^J(u^*)$ is in [0,1] and hence $u^* = \Gamma^J(u^*)$. □

It is important to notice that if $A_i(u) - I_i(u) > 0$ then $\Gamma_i^J(u)$ (which is well-defined for $J$ small) converges to 1 and if $A_i(u) - I_i(u) < 0$ then $\Gamma_i^J(u)$ converges to 0 as $J \to 0$. Hence, $\Gamma^J(u)$ converges pointwise to $H(Wu + b)$ on $\cup_{\mathscr{C}\in\Omega}\mathscr{C}$ as $J \to 0$. The next lemma states that for any compact subset of $\cup_{\mathscr{C}\in\Omega}\mathscr{C}$ we have uniform convergence and that the derivative of this function converges uniformly to zero.

**Lemma 12**

If $K$ is a compact subset of $\cup_{\mathscr{C}\in\Omega}\mathscr{C}$, then

- The function $\Gamma^J$ converges uniformly to the function $u \mapsto H(Wu + b)$ on $K$ as $J \to 0$. In particular, since $H(Wu + b)$ is constant in each chamber, we get that for any chamber $\mathscr{C} \in \cup_{\mathscr{C}\in\Omega}\mathscr{C}$, $\Gamma^J$ converges uniformly to the constant function $H(Wv + b)$ on $K \cap \mathscr{C}$ for any fixed $v \in C$. Also, $\Gamma^J$ converges uniformly to the constant function $H(Wx + b)$ on $K \cap \mathscr{C}(x)$ for any $x \in \{0,1\}^N$
- The Jacobian matrix $D\Gamma^J$ converges uniformly to zero on $K$ as $J \to 0$.

**Proof—**Similar to the proof of Lemma 11, there is a number $r > 0$ such that $|A_i(u) - I_i(u)| \geq r$ for all $i$ and for all $u \in K$, which is enough to guarantee uniform convergence on $K$. □

We now prove Theorem 4

**Proof—**In this proof, "ODE" will refer to the ODE in Eq. (1) and "BN" will refer to the BN in Eq. (17). Even though the steady states of this ODE depend on $J$, for simplicity we will denote them by $u^*$ instead of $u^{*J}$.

First, from Lemma 11 we consider $\in_K > 0$ such that for all $0 < J < \in_K$ the function $\Gamma^J$ is well-defined on $K$ and such that $u^* \in K$ is a steady state of the ODE if and only if $u^*$ is a fixed point of $\Gamma^J$. Second, from Lemma 12 we have that $\Gamma^J$ converges uniformly to the constant vector $h(x) = H(Wx + b)$ on $K \cap \mathscr{C}(x)$. Since $h(x)$ is in $\{0, 1\}^N$, we have that $K \cap \mathscr{C}(h(x))$ contains a neighborhood of $h(x)$. It follows from uniform convergence that for all $0 < J < \in_K$ (taking a smaller $\in_K$ if necessary), $\Gamma^J(K \cap \mathscr{C}(x)) \subseteq K \cap \mathscr{C}(\mathrm{h}(x))$. Also, on any chamber $\mathscr{C}$ that does not contain an element of $\{0, 1\}^N$, $\Gamma^J$ converges uniformly to the constant vector $x := H(Wv + b)$ for any fixed $v \in \mathscr{C}(H(Wu+b) \text{ is constant on } \mathscr{C})$; then, for all $0 < J < \in_K$ (taking a smaller $\in_K$ if necessary) $\Gamma^J(K \cap \mathscr{C}) \subseteq K \cap \mathscr{C}(x)$. Also note that $K \cap \mathscr{C}$ is compact for any chamber $\mathscr{C}$.

Now, suppose $x^*$ is a steady state of the BN, that is, $h(x^*) = x^*$. Then, for all $0 < J < \in_K$ we obtain that $\Gamma^J(K \cap \mathscr{C}(x^*)) \subseteq K \cap \mathscr{C}(h(x^*)) = K \cap \mathscr{C}(x^*)$. Since we have a continuous function from a convex compact set to itself, $\Gamma^J$ has a fixed point $\Gamma^J(u^*) = u^* \in K \cap \mathscr{C}(x^*)$. Then, $u^* \in K \cap \mathscr{C}(x^*)$ is a steady state of the ODE. Now suppose that the ODE has a steady state $u^* \in K$, and let $\mathscr{C}$ be the chamber that contains $u^*$ and $x^* := H(Wu^* + b)$. Since $u^* = \Gamma^J(u^*) \in \Gamma^J(K \cap \mathscr{C}) \subseteq K \cap \mathscr{C}(x^*)$, we have that $u^* \in \mathscr{C}(x^*)$. Since $u^*$ and $x^*$ belong to the same chamber we also have that $H(Wx^* + b) = H(Wu^* + b) = x^*$; thus, $x^*$ is a steady state of the BN.

From Lemma 12 we can make the norm of $D\Gamma^J$ small so that $u^*$ is the unique fixed point of $\Gamma^J$ in $K \cap \mathscr{C}(x^*)$. Since $\Gamma^J$ converges uniformly to $H(Wx^*+b) = h(x^*) = x^*$ on $K \cap \mathscr{C}(x^*)$, we have that $u^* = \Gamma^J(u^*)$ converges to $x^*$. Finally, to prove that the steady state of the ODE is asymptotically stable, we will show that the Jacobian matrix of the ODE can be seen as a small perturbation of a matrix that has negative eigenvalues. We will use the alternative form of $\Gamma_i^J$:

$$\Gamma_1^J(u) = \frac{2A_i(u)J}{-A_i(u)+I_i(u)+A_i(u)J+I_i(u)J+\sqrt{\Delta_i(u)}}.$$

Denote $f^J = (f_1^J, \ldots, f_N^J)$ where $f_i^J(u) = A_i(u)\frac{1-u_i}{J+1-u_i} - I_i(u)\frac{u_i}{J+u_i}$. We now compute $Df(u)$. For $i \neq j$ we have

$$\frac{\partial f_i^J}{\partial u_j} = w_{ij}^+ \frac{1-u_i}{J+1-u_i} - w_{ij}^- \frac{u_i}{J+u_i}.$$

Also,

$$\frac{\partial f_i^J}{\partial u_i}=w_{ii}^+\frac{1-u_i}{J+1-u_i}-w_{ii}^-\frac{u_i}{J+u_i}-A_i(u)\frac{J}{(J+1-u_i)^2}-I_i(u)\frac{J}{(J+u_i)^2}.$$

Let $Z^J$ be the matrix given by $Z_{ij}^J=w_{ij}^+\frac{1-u_i}{J+1-u_i}-w_{ij}^-\frac{u_i}{J+u_i}$ and denote with $E^J$ the diagonal matrix with entries $E_{ii}^J=-A_i(u)\frac{J}{(J+1-u_i)^2}-I_i(u)\frac{J}{(J+u_i)^2}$. Then,

$$Df^J(u)=Z^J+E^J$$

where the entries of $Z^J$ are bounded and $E^J$ is a diagonal matrix. We now will show that for any steady state of the ODE in $K$, $\lim_{J\to 0}E_{ii}^J=-\infty$ as $J\to 0$. After showing this, we can see $Df^J(u^*)$ as a small perturbation of a matrix that has negative eigenvalues. Since eigenvalues are continuous with respect to matrix entries, it follows that the eigenvalues of $Df^J(u^*)$ have negative real part, and hence, $u^*$ is asymptotically stable.

We now show that $\lim_{J\to 0}E_{ii}^J=-\infty$ as $J\to 0$. By computing $\frac{(\Gamma_i^J(u))^2}{J}$ and setting $J=0$, it follows that $\lim_{J\to 0}\frac{(\Gamma_i^J(u))^2}{J}=0$ when $A_i(u)-I_i(u)$ is negative. Similarly, we obtain that $\lim_{J\to 0}\frac{(1-\Gamma_i^J(u))^2}{J}=0$ when $A_i(u)-I_i(u)$ is positive. From these two limits, it follows that if $|A_i(u)-I_i(u)|\neq 0$, then $\lim_{J\to 0}\frac{(J+\Gamma_i^J(u))^2}{J}=0$ or $\lim_{J\to 0}\frac{(J+1-\Gamma_i^J(u))^2}{J}=0$ Furthermore, since $A_i(u)-I_i(u)$ is uniformly nonzero on $K$, the convergence is uniform.

If $u^*\in K$ is a steady state of the ODE, then $u_i^*=\Gamma^J(u^*)$ and

$\lim_{J\to 0}\left(-A_i(u)\frac{J}{(J+1-u_i^*)^2}-I_i(u)\frac{J}{(J+u_i^*)^2}\right)=\lim_{J\to 0}\left(-A_i(u)\frac{J}{(J+1-\Gamma_i^J(u^*))^2}-I_i(u)\frac{J}{(J+\Gamma_i^J(u^*))^2}\right)=$
Note that uniform convergence is needed in the last step because $u^*$ depends on $J$. □

## 6.4 Proof of Theorems 6 and 8

In the rest of this section, “ODE” will refer to the ODE in Eq. (1) and “BN” will refer to the BN in Eq. (17).

Notice that for any $x\in\{0,1\}^N$, $\mathscr{C}(x)=\{u\in[0,1]^N:H(Wu+b)=H(Wx+b)\}$. We now prove Theorem 6.

**Proof—**Let $y=h(x)$ and for simplicity in the notation, assume that $y=(0,\ldots,0)$.

In the case $x = y$, we will show that (0,…,0) contains an invariant set for the original ODE. Since $x = (0,\ldots,0)$ and $h(x) = x$, we have that $\mathscr{C}(x)=\cap_{i=1}^{N}\{u \in [0,1]^N:\sum_{j=1}^{N} w_{ij}u_j+b_i<0\}$. We now consider a hypercube of the form $K = [0, D]^N$ with $D$ small so that $K \subseteq \mathscr{C}(x)$. We claim that for $J$ small $K$ is invariant. Since we already showed that $[0, 1]^N$ is invariant, it is enough to check that if $u \in K$ with $u_i = D$, then $f_i^J(u) \leq 0$. Since $K$ is compact and $\sum_{j=1}^{N} w_{ij}u_j+b_i<0$ for all $i$ and for all $u \in K$, there is $r > 0$ such that $\sum_{j=1}^{N} w_{ij}u_j+b_i \leq -r$ all $u \in K$. It follows that $A_i(u) - I_i(u)\frac{u_i}{J+u_i}$ converges uniformly to $A_i(u) - I_i(u)=\sum_{j=1}^{N} w_{ij}u_j+b_i \leq -r$ on $\{u \in K : u_i = D\}$ as $J \to 0$. Also, $f_i^J(u)=A_i(u)\frac{1-u_i}{J+1-u_i} - I_i(u)\frac{u_i}{J+u_i} \leq A_i(u) - I_i(u)\frac{u_i}{J+u_i}$ on $\{u \in K : u_i = D\}$. Thus, on $\{u \in K : u_i = D\}$, $f_i^J$ is bounded above by a function that converges uniformly to a negative function. Then, there is $\in_K > 0$ such that for all $0 < J < \in_K$, $f_i^J$ is negative on $\{u \in K : u_i = D\}$. Then, $K$ is invariant.

In the case $x \neq y$, we assume for simplicity that $x = (1, 0,\ldots,0)$ and $y = (0, 0,\ldots,0)$. Then, since $h(x) = y$ and $h_1(y) = 0$, we have the following

$$\sum_{j=1}^{N} w_{ij}u_j+b_i<0, \text{ for all } u \in \mathscr{C}(x), \text{ and } \sum_{j=1}^{N} w_{1j}u_j+b_1<0, \text{ for all } u \in \mathscr{C}(y).$$

In particular, $\sum_{j=1}^{N} w_{1j}u_j+b_1<0$ for all $u \in \mathscr{C}(x) \cup \mathscr{C}(y)$. This also means that the hyperplane that separates $\mathscr{C}(x)$ and $\mathscr{C}(y)$ is $\{u:\sum_{j=1}^{N} w_{kj}u_j+b_k=0\}$ for some $k \neq 1$; then, the common face of $\mathscr{C}(x)$ and $\mathscr{C}(y)$ is given by

$$\{u \in [0,1]^N:\sum_{j=1}^{N} w_{ij}u_j+b_i<0 \text{ for } i \neq k \text{ and } \sum_{j=1}^{N} w_{kj}u_j+b_k=0\}.$$

Now, for $r > 0$ small, we define the set

$$L:=\{u \in [0,1]^N:\sum_{j=1}^{N} w_{ij}u_j+b_i< -r \text{ for } i \neq k \text{ and } \sum_{j=1}^{N} w_{kj}u_j+b_k=0\}$$

which will be a face of the neighborhood of $x$ that we are looking for (see Fig. 11). We now project $L$ onto the $u_1 = 0$ plane (see Fig. 11); that is, define

$$L_1:=\{(0, u_2, u_3, \ldots, u_N):(u_1, \ldots, u_N) \in L \text{ for some } u \in L\}$$

We use $L_1$ to “generate” a box parallel to the $u_1$ axis (see Fig. 11); namely, consider

$$B:=\{u\in[0,1]^N:(0,u_2,\ldots,u_N)\in L_1\}.$$

Now, consider the neighborhood of $x$ given by

$$K:=B\cap\mathscr{C}(x).$$

$K$ is a polytope such that $L$ is one of its faces. Similar to the case $x = y$, there is $\in_K > 0$ such that for all $0 < J < \in_K$ we have that for any face of $K$ other than $L$ the vector field points inward. Also, the first coordinate of the vector field is negative on $K$. Thus, any solution with initial condition in $K$, must exit $K$ through its face $L$ and then enter $\mathscr{C}(y)$. That is, the ODE transitions from $K$ to $\mathscr{C}(y)$. □

We prove Theorem 8.

**Proof—**We proceed as in the proof of Theorem 6 and for simplicity we assume that $x = (1,0,\ldots,0)$ and $y = h(x) = (0,\ldots,0)$. Since $h(x) = y$ and $h_1(y) = 0$, we have the following

$$\sum_{j=1}^{N}w_{ij}u_j+b_i<0,\text{ for all }u\in\mathscr{C}(x),\text{ and }\sum_{j=1}^{N}w_{1j}u_j+b_1<0,\text{ for all }u\in\mathscr{C}(y).$$

In particular, $\sum_{j=1}^{N}w_{1j}u_j+b_1<0$ for all $u\in\mathscr{C}(x)\cup\mathscr{C}(y)$. This also means that the hyperplane that separates $\mathscr{C}(x)$ and $\mathscr{C}(y)$ is $\{u:\sum_{j=1}^{N}w_{kj}u_j+b_k=0\}$ for some $k \neq 1$; furthermore, since this hyperplane is parallel to the axes, we have that $(w_{k1}, w_{k2},\ldots,w_{kN}) = (w_{k1}, 0,\ldots,0)$. Then, the hyperplane that separates $\mathscr{C}(x)$ and $\mathscr{C}(y)$ is $\{u:u_1=\frac{b_k}{-w_{k1}}\}$ and the common face of $\mathscr{C}(x)$ and $\mathscr{C}(y)$ is given by

$$\{u\in[0,1]^N:\sum_{j=1}^{N}w_{ij}u_j+b_i<0\text{ for }i\neq k\text{ and }u_1=\frac{b_k}{-w_{k1}}\}.$$

Now, let $K$ be a compact subset of $\mathscr{C}(x)$ and consider $r > 0$ small such that $K\subseteq K^0:=\{u\in[0,1]^N:\sum_{j=1}^{N}w_{ij}u_j+b_i\leq -r\text{ for }i\neq k\text{ and }u_1\geq\frac{b_k}{-w_{k1}}\}$ (see Fig. 12). Since the hyperplanes in $\mathscr{H}$ are parallel to the axis, $K^0$ is a box with faces parallel to the axes and $K^0$ also shares a face with $\mathscr{C}(y)$. Then, similar to the proof of Theorem 6, there is $\in_K > 0$ such that for all $0 < J < _K$ we have that at the faces of $K^0$ other than that face shared with $\mathscr{C}(y)$, the vector field of the ODE points inward, and the first entry of the vector field is negative. Then, the ODE will transition from $K^0$ to $\mathscr{C}(y)=\mathscr{C}(h(x))$.

Now, let $K^1$ be a compact subset of $\mathscr{C}(h(x))$ such that $K^1$ intersects all solutions that start in $K$ (see Fig. 12). Then, for all $0 < J < \in_K$ (making $\in_K$ smaller if necessary) the ODE

transitions from $K^1$ to $\mathscr{C}(h^2(x))$. This also means that the ODE transitions from $K^0$ to $\mathscr{C}(h^2(x))$. The proof follows by induction. □

## 6.5 Case $n > 1$

In this case, Eq. (1) becomes

$$\frac{du_i}{dt}=A_i\frac{(1-u_i)^n}{J^n+(1-u_i)^n}-I_i\frac{u_i^n}{J^n+u_i^n}.$$

The behavior of the system as $J \to 0$ is similar. To illustrate this, we use the example from Section 6.2 for $n > 1$; namely, consider

$$\frac{dx}{dt}=A\frac{(1-x)^n}{J^n+(1-x)^n}-I\frac{x^n}{J^n+x^n}. \quad (26)$$

Fig. 13 shows the graph of the right hand side of Eq. (26) for the fixed values $A = 1$, $I = 0.5$, three different values of $J$, and three different values of $n$. Note that as $J$ becomes smaller, the graph gets flatter in (0,1) as in Section 6.2.

All definitions and results remain virtually unchanged except Sections 6.3 and 6.4. For $n > 1$ Eq. (23) becomes

$$A_i(u^*)\frac{(1-u_i^*)^n}{J^n+(1-u_i^*)^n}-I_i(u^*)\frac{(u_i^*)^n}{J^n+(u_i^*)^n}=0,$$

which cannot be solved in terms of $u_i^*$ in closed form as in Eq. (24) and Eq. (25). However, we can use the implicit function theorem to guarantee the existence of a function $\Gamma^J$ with the required properties (such as compact convergence to the Heaviside function).

## 6.6 Avoiding discontinuity of solutions in Eq. (14)

There is a way to make the approximations continuous, although it requires to change the equations in the boundary domains. The idea is to reduce the vector field using the approximations $u_t \approx 1$ and $u_s \approx 0$ where appropriate, while keeping the derivatives.

For example for the region $\mathscr{R}_{12}$ we keep the derivatives and just use $u_1 \approx 0$ and $u_2 \approx 0$ in the right hand side of Eq. (2). This will yield

$$\begin{aligned}\tfrac{du_1}{dt}&=0.5,\\ \tfrac{du_2}{dt}&=0.5\end{aligned} \quad (27)$$

This is still a decoupled system and solvable.

Similarly for region $\mathscr{R}^{12}$, using $u_1 \approx 1$, $u_2 \approx 1$, we will get

$$\begin{aligned}\frac{du_1}{dt}&=0.5\frac{1-u_1}{J+1-u_1}-1,\\ \frac{du_2}{dt}&=0.5\frac{1-u_2}{J+1-u_2}-1.\end{aligned} \quad (28)$$

This is also decoupled and solvable, though it is not linear.

For regions $\mathscr{R}_1^2$ ($u_1 \approx 0$, $u_2 \approx 1$) and $\mathscr{R}_2^1$ ($u_1 \approx 1$, $u_2 \approx 0$) we will get

$$\begin{aligned}\frac{du_1}{dt}&=0.5-\frac{u_1}{J+u_1},\\ \frac{du_2}{dt}&=0.5\frac{1-u_2}{J+1-u_2},\end{aligned} \quad (29)$$

and

$$\begin{aligned}\frac{du_1}{dt}&=0.5\frac{1-u_1}{J+1-u_1},\\ \frac{du_2}{dt}&=0.5-\frac{u_2}{J+u_2},\end{aligned} \quad (30)$$

respectively. These equations are again decoupled and solvable, but again we lost the linearity.

We see that in each corner our original system can be approximated with decoupled, solvable equations. A similar idea can be used for other regions, but as seen above, this alternative approach introduces nonlinearity.

## References


Abou-Jaoudé W, Ouattara D, Kaufman M. From structure to dynamics: frequency tuning in the p53-mdm2 network: I. logical approach. J Theor Biol. 2009; 258(4):561–577. [PubMed: 19233211]

Abou-Jaoudé W, Ouattara D, Kaufman M. From structure to dynamics: fre quency tuning in the p53-mdm2 network: II. differential and stochastic approaches. J Theor Biol. 2010; 264(4):1177–1189. [PubMed: 20346959]

Aguda, D. Modeling the Cell Division Cycle, Lecture Notes in Mathematics. Vol. 1872. Springer; 2006. p. 1-22.

Albert R, Othmer H. The topology of the regulatory interactions predicts the expression pattern of the segment polarity genes in Drosophila Melanogaster. J Theor Biol. 2003; 223(1):1–18. [PubMed: 12782112]

Alon, U. An Introduction to Systems Biology: Design Principles of Biological Circuits. Chapman and Hall/CRC; 2006.

Aracena J, Goles E, Moreira A, Salinas L. On the robustness of update schedules in Boolean networks. Biosystems. 2009; 97(1):1–8. [PubMed: 19505631]

Casey R, de Jong H, Gouzé J. Piecewise-linear Models of Genetic Regulatory Networks: Equilibria and their Stability. Journal of Mathematical Biology. 2006; 52(1):27–56. [PubMed: 16195929]

Chaves M, Tournier L, Gouzé J. Comparing Boolean and piecewise affine differential models for genetic networks. Acta Biotheoretica. 2010; 58(2):217–232. [PubMed: 20665073]

Cheng X, Sun M, Socolar J. Autonomous Boolean modelling of developmental gene regulatory networks. J R Soc Interface. 2013; 10(78):20120574. [PubMed: 23034351]

Ciliberto A, Capuani F, Tyson J. Modeling networks of coupled enzymatic reactions using the total quasi-steady state approximation. PLoS Computational Biology. 2007; 3(3):e45. [PubMed: 17367203]

Davidich M, Bornholdt S. The transition from differential equations to Boolean networks: A case study in simplifying a regulatory network model. J Theor Biol. 2008; 255(3):269–277. [PubMed: 18692073]

Davidich M, Bornholdt S. Boolean Network Model Predicts Cell Cycle Sequence of Fission Yeast. PLoS ONE. 2008; 3(2):e1672. [PubMed: 18301750]

De Jong H. Modeling and simulation of genetic regulatory systems: a literature review. Journal of Computational Biology. 2002; 9(1):67–103. [PubMed: 11911796]

De Jong H, Gouzé J, Hernandez C, Page M, Sari T, Geiselmann J. Qualitative simulation of genetic regulatory networks using piecewise-linear models. Bull Math Bio. 2004; 66(2):301–340. [PubMed: 14871568]

Edwards R, Siegelmann H, Aziza K, Glass L. Symbolic dynamics and computation in model gene networks. Chaos: An Interdisciplinary Journal of Nonlinear Science. 2001; 11(1):160–169.

Elowitz M, Leibler S. A synthetic oscillatory network of transcriptional regulators. Nature. 2000; 403(6767):335–338. [PubMed: 10659856]

Fenichel N. Geometric singular perturbation theory for ordinary differential equations. Journal of Differential Equations. 1979; 31(1):53–98.

Franke R, Theis F, Klamt S. From Binary to Multivalued to Continuous Models: The lac Operon as a Case Study. J Integrative Bioinformatics. 2010; 7(1):151.

Gardner T, Cantor C, Collins J. Construction of a genetic toggle switch in escherichia coli. Nature. 2000; 403(6767):339–342. [PubMed: 10659857]

Glass L, Kauffman S. The logical analysis of continuous, non-linear biochemical control networks. J Theor Biol. 1973; 39(1):103–129. [PubMed: 4741704]

Glass L. Classification of biological networks by their qualitative dynamics. J Theor Biol. 1975; 54(1): 85–107. [PubMed: 1202295]

Glass L. The logical analysis of continuous, non-linear biochemical control networks. Journal of Chemical Physics. 1975; 63(1):1325–1335.

Goldbeter A. A minimal cascade model for the mitotic oscillator involving cyclin and cdc2 kinase. Proceedings of the National Academy of Sciences of the United States of America. 1991; 88(20): 9107–9111. [PubMed: 1833774]

Goldbeter A, Koshland D. An amplified sensitivity arising from covalent modifi-cation in biological systems. Proceedings of the National Academy of Sciences of the United States of America. 1981; 78(11):6840–6844. [PubMed: 6947258]

Gouzé J, Saria T. A class of piecewise linear differential equations arising in biological models. Dynamical Systems. 2002; 17(4):299–316.

Hek G. Geometric singular perturbation theory in biological practice. Journal of Mathematical Biology. 2010; 60(3):347–386. [PubMed: 19347340]

Ironi L, Panzeri L, Plahte E, Simoncini V. Dynamics of actively regulated gene networks. Physica D. 2011; 240:779–794.

Ishii N, Suga Y, Hagiya A, Watanabe H, Mori H, Yoshino M, Tomita M. Dynamic simulation of an in vitro multi-enzyme system. FEBS Lett. 2007; 581(3):413–420. [PubMed: 17239859]

Kaper T. An introduction to geometrical methods and dynamical dystems for singular perturbation problems. Analyzing Multiscale Phenomena Using Singular Perturbation Methods: American Mathematical Society Short Course, January 5–6, 1998, Baltimore, Maryland (Proc Sym Ap). 1998:85–132.

Kauffman S. Metabolic stability and epigenesis in randomly constructed genetic nets. J Theor Biol. 1969; 22(3):437–467. [PubMed: 5803332]

Kumar A, Josić K. Reduced models of networks of coupled enzymatic reactions. J Theor Biol. 2011

Li F, Long T, Lu Y, Ouyang Q, Tang C. The yeast cell-cycle network is robustly designed. Proc Natl Acad Sci USA. 2004; 101(14):4781–4786. [PubMed: 15037758]

Ma W, Trusina A, El-Samad H, Lim W, Tang C. Defining network topologies that can achieve biochemical adaptation. Cell. 2009; 138(4):760–773. [PubMed: 19703401]

Mendoza L, Xenarios I. A method for the generation of standardized qualitative dynamical systems of regulatory networks. Theoretical Biology and Medical Modelling. 2006; 3(13):1–18. [PubMed: 16403216]

Michaelis L, Menten M. Die kinetik der inwertin wirkung. Biochemische Zeitschrift. 1913; 49:333–369.

Mochizuki A. An analytical study of the number of steady states in gene regulatory networks. J Theor Biol. 2005; 236:291–310. [PubMed: 15885706]

Novak B, Csikasz-Nagy A, Gyorffy B, Chen K, Tyson JJ. Mathematical model of the ssion yeast cell cycle with checkpoint controls at the G1/S, G2/M and metaphase/anaphase transitions. Biophysical Chemistry. 1998; 72:185–200. [PubMed: 9652094]

Novak B, Tyson JJ. Numerical analysis of a comprehensive model of m-phase control in xenopus oocyte extracts and intact embryos. Journal of Cell Science. 1993; 106(4):1153–1168. [PubMed: 8126097]

Novak B, Pataki Z, Ciliberto A, Tyson J. Mathematical model of the cell division cycle of fission yeast. Chaos (Woodbury, NY). 2001; 11(1):277–286.

Polynikis A, Hogan SJ, di Bernardo M. Comparing different ODE modelling approaches for gene regulatory networks. J Theor Biol. 2009; 261(4):511–530. [PubMed: 19665034]

Snoussi E. Qualitative dynamics of piecewise differential equations: a discrete mapping approach. Dynamics and Stability of Systems. 1989; 4(3):189–207.

Sun M, Cheng X, Socolar J. Causal structure of oscillations in gene regulatory networks: Boolean analysis of ordinary differential equation attractors. Chaos. 2013; 23(2):025104. [PubMed: 23822502]

Thomas, R.; D'Ari, R. Biological Feedback. CRC; 1990.

Tyson J, Chen K, Novak B. Sniffers, buzzers, toggles and blinkers: dynamics of regulatory and signaling pathways in the cell. Current Opinion in Cell Biology. 2003; 15(2):221–231. [PubMed: 12648679]

van Zwieten D, Rooda J, Armbruster D, Nagy J. Simulating feedback and reversibility in substrate-enzyme reactions. Eur Phys J B. 2011; 84:673–684.

Veliz-Cuba A, Arthur J, Hochstetler L, Klomps V, Korpi E. On the Relationship of Steady States of Continuous and Discrete Models Arising from Biology. Bull Math Bio. 2012; 74(12):2779–2792. [PubMed: 23081727]

Verhulst, F. Methods and applications of singular perturbations. Springer; 2005.

Wittmann D, Krumsiek J, Saez-Rodriguez J, Lauffenburger D, Klamt S, Theis F. Transforming Boolean models to continuous models: methodology and application to T-cell receptor signaling. BMC Systems Biology. 2009; 3(1):98. [PubMed: 19785753]

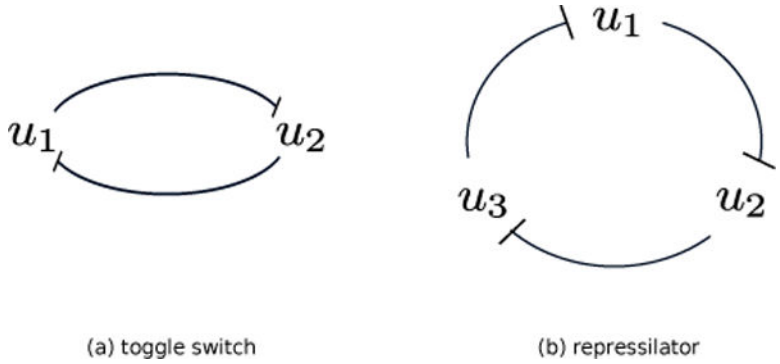


**Figure 1.**
(a) Nodes $u_1$, $u_2$ inhibiting each other's activity resulting in a switch. The node which starts out stronger suppresses the activity of the other. (b) Nodes $u_1$, $u_2$, and $u_3$ suppress each other in a cyclic fashion. Under certain conditions, this can lead to oscillations.

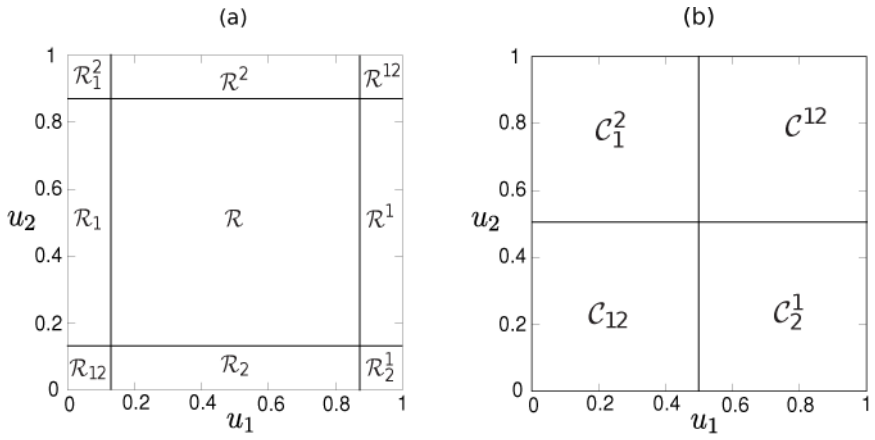


**Figure 2.**

Subdomains $\mathscr{R}_S^T$ for the unit square $[0, 1]^2$ (panel a), and chambers of $[0, 1]^2$ defined by the asymptotic behavior of the nullclines of Eq. (2) (panel b).

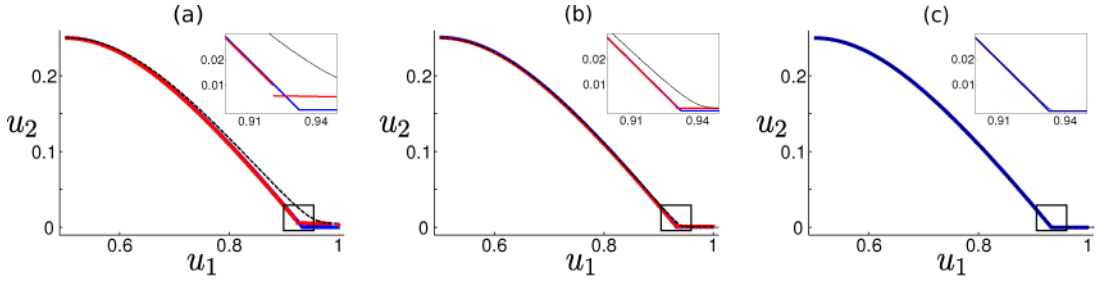


**Figure 3.**

Comparison of the numerical solution of Eq. (2) (dashed black) with the solution of the approximate system as listed in Table 1 (red) for two different values of $J$ (panels (a) and (b)) and the 0-th order approximation (blue). We used $J = 5 \times 10^{-3}$ in (a), $J = 10^{-3}$ in (b), and $J = 10^{-4}$ in (c). We also used $\delta = 2J$. (a,b) The solution of the linear approximation started in the subdomain $\mathscr{R}$ (Initial value: $u_1 = 0.5$, $u_2 = 0.25$), and as soon as $u_2$ decreased below $\delta$, we assumed that the solution entered subdomain $\mathscr{R}_2$. The approximate solution is discontinuous since when $u_2 = \delta$, the solution jumped (see inset) to the manifold, described by the algebraic part of the linear differential algebraic system prevalent in the subdomain $\mathscr{R}_2$, Eq. (7b). The solution finally stopped in the subdomain $\mathscr{R}_2^1$. As $J$ gets smaller, the discontinuity becomes negligible and the approximate system from Table 1 converges to the (continuous) 0-th order approximation. (c) The 0-th order approximation (black solid curve) becomes an accurate approximation of the original system as $J \to 0$ (the solution from Table 1 is not shown in panel (c)).

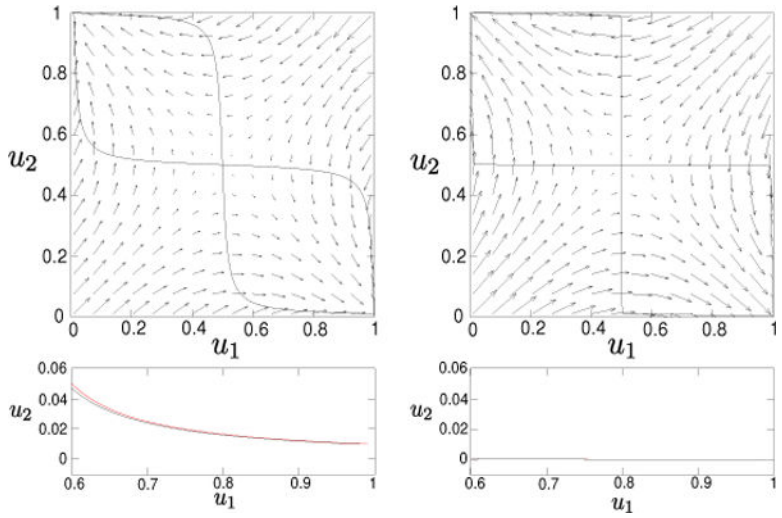


**Figure 4.**

Behavior of nullclines as $J$ decreases. Top: Nullclines of Eq. (2) for $J = 10^{-2}$ (left) and $J = 10^{-4}$ (right). Bottom: Nullcline $\frac{du_2}{dt}=0$ of Eq. (2) (black curve) and the manifold defined by Eq. (7b) (red) for $J = 10^{-2}$ and $\delta = 10^{-}2$ (left), and $J = 10^{-4}$ and $\delta = 10^{-}2$ (right).

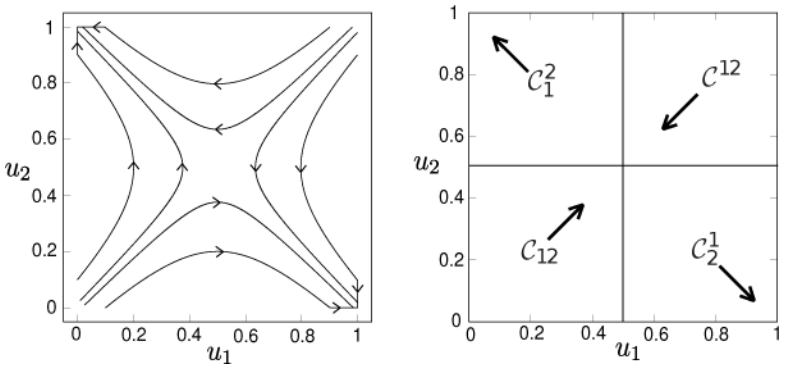


**Figure 5.**

Left: Solutions of Eq. (2) for $J = 10^{-4}$. When a solution is close to the boundary regions of $\mathscr{C}_1^2$ and $\mathscr{C}_2^1$, they enter the invariant region as shown in Fig. 3b. Right: Graphical representation of the Boolean transitions ($00 \to 11$, $11 \to 00$, $01 \to 01$, $10 \to 10$).

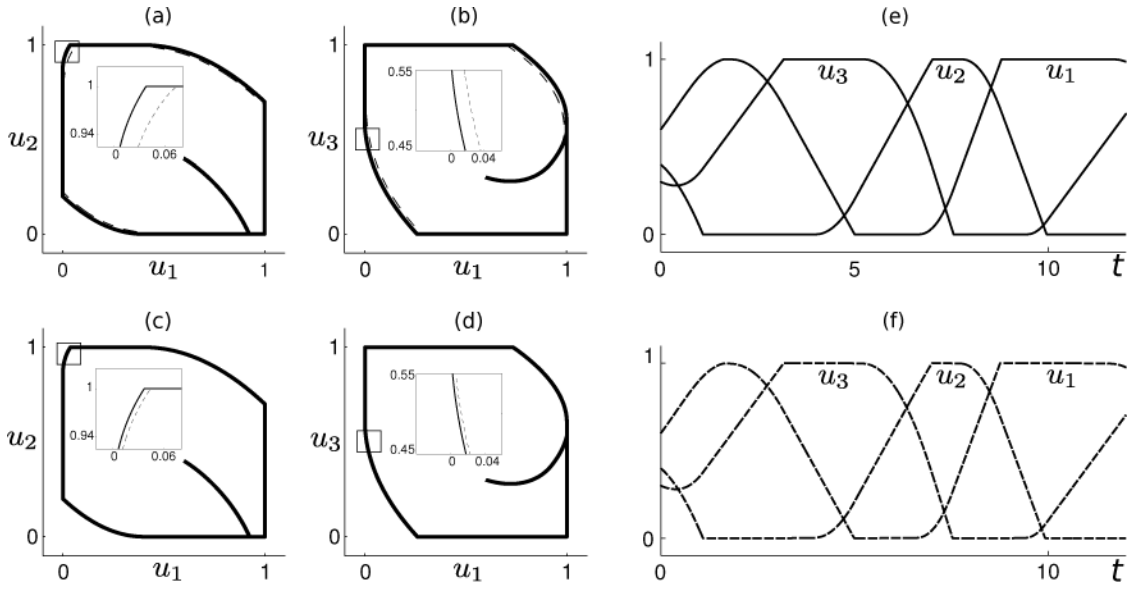


**Figure 6.**

Comparison of the numerical solution of Eq. (10) (dashed black) and the 0-th order approximation (solid black curves) for two different values of $J$. For (a)–(b) $J = 10^{-3}$; for (c)–(d) $J = 10^{-4}$. Panel (e) shows the time series for the 0-th order approximation. Panel (f) shows the time series for the solutions of Eq. (10) using $J = 10^{-4}$.

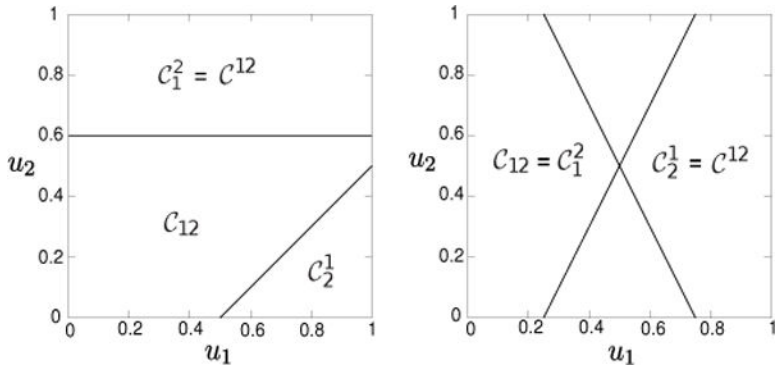


**Figure 7.**

chambers for $W = \begin{bmatrix} 1 & -1 \\ 0 & -1 \end{bmatrix}$ and $b = \begin{bmatrix} -0.5 \\ 0.6 \end{bmatrix}$ (left); $W = \begin{bmatrix} 2 & -1 \\ 2 & 1 \end{bmatrix}$ and $b = \begin{bmatrix} -0.5 \\ -1.5 \end{bmatrix}$

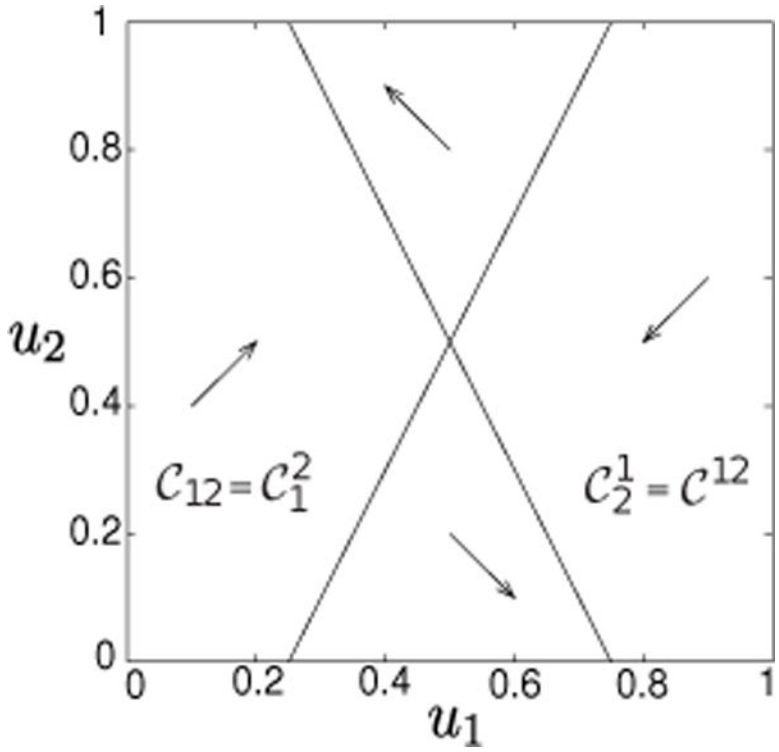


**Figure 8.**

Chambers and signs of vector field for the linear system given by $W = \begin{bmatrix} -2 & -1 \\ -2 & 1 \end{bmatrix}$ and $b = \begin{bmatrix} 1.5 \\ 0.5 \end{bmatrix}$.

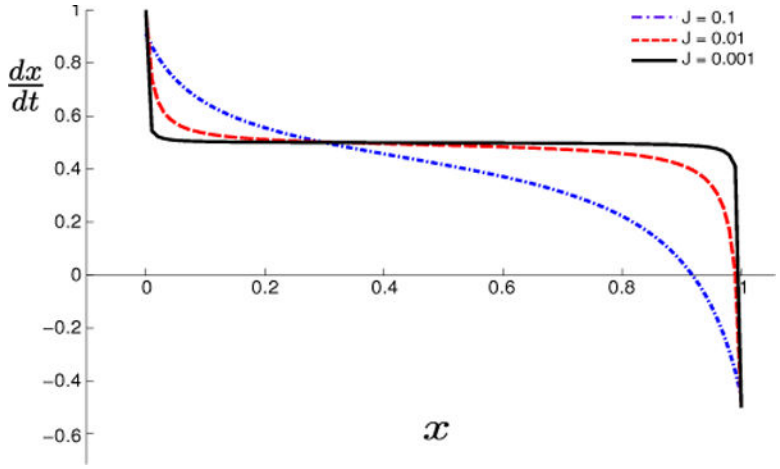


**Figure 9.**

Plots of right hand side of Eq. (22) for three different values of *J*, as functions of *x*. Other parameters: $A = 1$, $I = .5$. This figure suggests that differential equations of the form Eq. (22) can be approximated by linear ODEs in the interior of the domain.

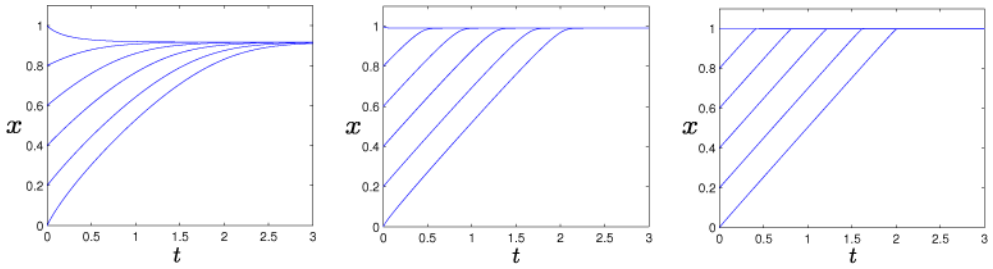


**Figure 10.**

Solutions of Eq. (22) for three different values of $J$ (left: $J = 0.1$, center: $J = 0.01$, right: $J = 0.001$). Other parameters: $A = 1$, $I = .5$.

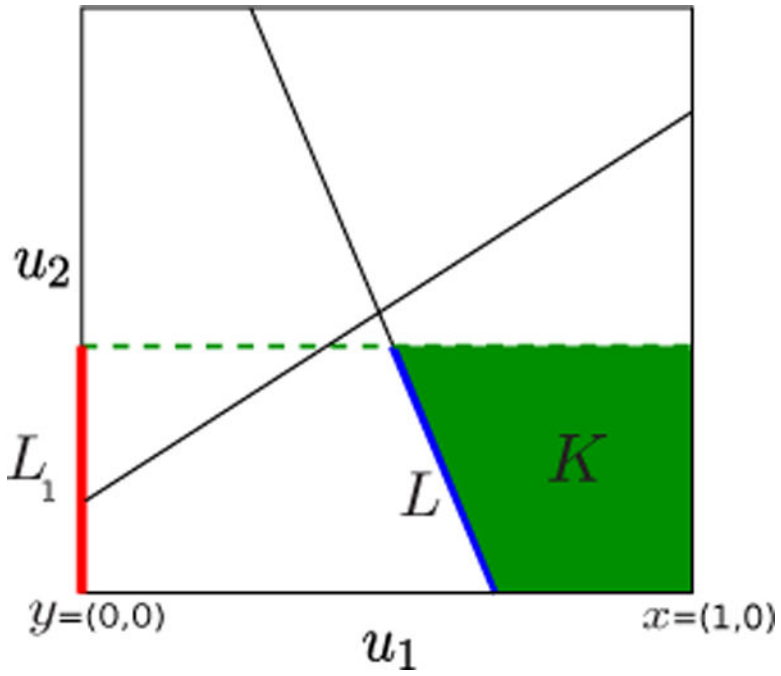


**Figure 11.**
Sets $L$ (blue), $L_1$ (red), and $K$ (green) in the proof of Theorem 6 for $N = 2$.

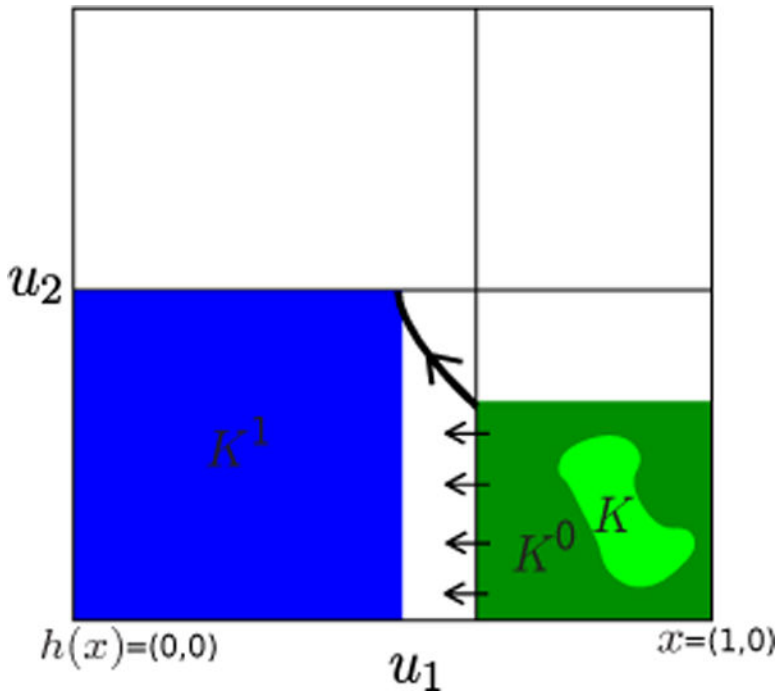


**Figure 12.**
Sets $K$ (light green), $K^0$ (dark green and light green), and $K^1$ (blue) in the proof of Theorem 8 for $N = 2$.

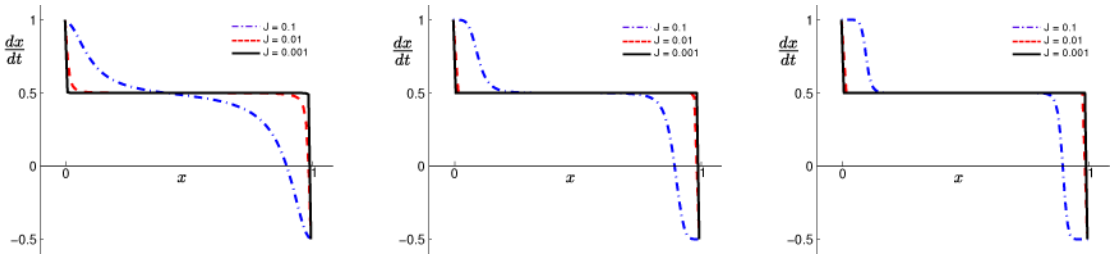


**Figure 13.**

Plots of right hand side of Eq. (26) for three different values of *J*, as functions of *x*, and three different values of *n* (left: *n* = 2, center *n* = 5, right: *n* = 10). Other parameters: *A* = 1, *I* = .5.

**Table 1**

A list of differential–algebraic systems that approximate Eq. (2) in different parts of the domain. The subdomains are named so that the superscript (subscript) lists the coordinates that are close to 1 (close to 0). For example, $\mathscr{R}_1^2$ denotes the subdomain with $u_1 \approx 0$ and $u_2 \approx 1$, and $\mathscr{R}^2$ the subdomain where $u_2$ is near 1, but $u$ is away the $\approx$ from boundary. The middle column gives the differential-algebraic system that approximates Eq. (2) within the given subdomain.

| Subdomain | Approximation using Eq. (14) | Alternative approximation (Section 6.6) |
|---|---|---|
| $\mathscr{R}$ | $u_1'=0.5-u_2,$<br>$u_2'=0.5-u_1$ | same<br>same |
| $\mathscr{R}^1$ | $0=0.5\frac{1-u_1}{J+1-u_1}-u_2,$<br>$u_2'=-0.5$ | $u_1'=0.5\frac{1-u_1}{J+1-u_1}-u_2,$<br>same |
| $\mathscr{R}^2$ | $u_1'=-0.5,$<br>$0=0.5\frac{1-u_2}{J+1-u_2}-u_1$ | same<br>$u_2'=0.5\frac{1-u_2}{J+1-u_2}-u_1$ |
| $\mathscr{R}_1$ | $0=0.5-u_2\frac{u_1}{J+u_1},$<br>$u_2'=0.5$ | $u_1'=0.5-u_2\frac{u_1}{J+u_1},$<br>same |
| $\mathscr{R}_2$ | $u_1'=0.5,$<br>$0=0.5-u_1\frac{u_2}{J+u_2}$ | same<br>$u_2'=0.5-u_1\frac{u_2}{J+u_2}$ |
| $\mathscr{R}^{12}$ | no solution,<br>no solution | $u_1'=0.5\frac{1-u_1}{J+1-u_1}-1,$<br>$u_2'=0.5\frac{1-u_2}{J+1-u_2}-1$ |
| $\mathscr{R}_{12}$ | no solution,<br>no solution | $u_1'=0.5,$<br>$u_2'=0.5$ |
| $\mathscr{R}_2^1$ | $0=0.5\frac{1-u_1}{J+1-u_1},$<br>$0=0.5-\frac{u_2}{J+u_2}$ | $\frac{du_1}{dt}=0.5\frac{1-u_1}{J+1-u_1},$<br>$\frac{du_2}{dt}=0.5-\frac{u_2}{J+u_2}$ |
| $\mathscr{R}_1^2$ | $0=0.5-\frac{u_1}{J+u_1},$<br>$0=0.5\frac{1-u_2}{J+1-u_2}$ | $u_1'=0.5-\frac{u_1}{J+u_1},$<br>$u_2'=0.5\frac{1-u_2}{J+1-u_2}$ |